TREE-RING RECONSTRUCTED STREAMFLOW AND DROUGHT HISTORY FOR

THE BIGHORN RIVER BASIN, WYOMING

by

Bryan Cameron Swindell

A thesis submitted in partial fulfillment
of the requirements for the degree

of

Master of Science

in

Earth Sciences

MONTANA STATE UNIVERSITY
Bozeman, Montana

November 2011

APPROVAL

of a thesis submitted by

Bryan Cameron Swindell

This thesis has been read by each member of the thesis committee and has been found to be satisfactory regarding content, English usage, format, citation, bibliographic style, and consistency and is ready for submission to The Graduate School.

Dr. Cathy Whitlock

Approved for the Department of Earth Sciences

Dr. Stephan Custer

Approved for The Graduate School

Dr. Carl A. Fox

## STATEMENT OF PERMISSION TO USE

In presenting this thesis in partial fulfillment of the requirements for a master's degree at Montana State University, I agree that the Library shall make it available to borrowers under rules of the Library.

If I have indicated my intention to copyright this thesis by including a copyright notice page, copying is allowable only for scholarly purposes, consistent with "fair use" as prescribed in the U.S. Copyright Law. Requests for permission for extended quotation from or reproduction of this thesis in whole or in parts may be granted only by the copyright holder.

Bryan Cameron Swindell

November 2011

ACKNOWLEDGEMENTS

TABLE OF CONTENTS

TABLE OF CONTENTS CONTINUED

## LIST OF TABLES

viii

LIST OF FIGURES

ABSTRACT

Predictions made by climate models suggest that in the coming decades the western United States will experience warmer temperatures, as well as changes in streamflow patterns.  To better understand how climatic variability affects water resources and to critique current water-supply assumptions, water-resource management can benefit from proxy-based paleoclimatic information.  Instrumental records of precipitation, streamflow, and snowpack are typically less than 100 years long and usually only capture a subset of the full range of hydrologic variability possible in a given watershed.  This study presents water-year streamflow reconstructions for six gages in the Bighorn River Basin in Wyoming and Montana. The reconstructions are based on tree-ring data from various locations in the Northern Rocky Mountain region.  The streamflow reconstructions are between 500 and 800 years long. Calibration models between the tree-ring data and the gage record explain up to 60% of the variation in gaged streamflow.  Analysis of the reconstructions indicates that the 20$^{th}$ century was relatively wet compared with previous centuries, and recent droughts were matched or exceeded (in duration and magnitude) many times during the last 800 years.  Pre-instrumental droughts also show strong spatial coherence across the entire Bighorn River watershed.  These reconstructions can be used to develop more-robust water-management plans that take into account a broader range of conditions than those presented by gage records alone.

## 1. INTRODUCTION

Current demands on water resources in the western United States will most likely not be met under plausible future climatic conditions (Barnett et al., 2004). Future climate is likely to include warmer temperatures, which will translate into diminished snowfall and earlier peak runoff in mountainous regions. In basins that depend on protracted spring and summer snowmelt, climate variability is likely to lead to conflicts between human demands and ecosystem requirements. Arid watersheds, such as the Bighorn River Basin of north-central Wyoming and south-central Montana, are especially sensitive to changes in water supply. Hydroclimatic variability, especially when combined with the effects of changing land-use patterns and economic structures, has the potential to significantly complicate water management. For these reasons, understanding the long-term nature of hydrologic variability is critical to managing water supplies in the future.

Water-resources management and planning are typically based on the instrumental record of watershed hydrology (WWDC, 2010). It is assumed that the data offered by precipitation, streamflow, and snowpack gages are representative of the full range of hydrologic variability possible in a given area. However, few such records extend beyond 100 years, and most span only the past 50 years. Paleoclimatic studies have shown that the 20th century instrumental record provides only a subset of the full range of hydroclimatic variability characteristic of western North America (Stockton and Jacoby, 1976; Meko et al., 1995; Gray et al., 2004; Barnett et al., 2010). Tree-ring analysis has emerged as a way to put 20th century hydroclimatic variability into a broader

context and determine the extent to which the instrumental record is representative of
long-term conditions. Precisely-dated annual growth rings from long-lived trees provide
a reliable hydroclimatic proxy that can extend hundreds or thousands of years beyond the
instrumental record (Meko et al., 1995). Carefully-analyzed data from moisture-sensitive
trees preserve both high- and low-frequency hydroclimatic variability and have been used
to estimate past streamflow with a high level of accuracy (Cook and Kairiukstis, 1990;
Loaiciga, 1993; Bonin and Burn, 2005). Insights gained from such reconstructions help
water managers plan for a wider range of water-supply scenarios than those found in the
instrumental record, and they offer a means of evaluating the assumptions made by
current water-management systems.

The objectives of this study were to address the following questions: Can the
Northern Rockies tree-ring chronology network be used to reconstruct streamflow in the
Bighorn River Basin? If so, what do the reconstructions reveal about the temporal and
spatial nature of drought over the past several centuries? Does streamflow show strong
correlations with oceanic climate variability, suggesting the possibility of long-lead
hydrologic forecasting? Finally, what does the new information about hydrologic
variability offer water management in the Basin, especially considering a warming
climate?

In this thesis, I first present tree-ring-based streamflow reconstructions for
selected portions of the Bighorn River Basin, including the Wind River portion of the
watershed (Figure 1). Water-year (October through September) total streamflow was
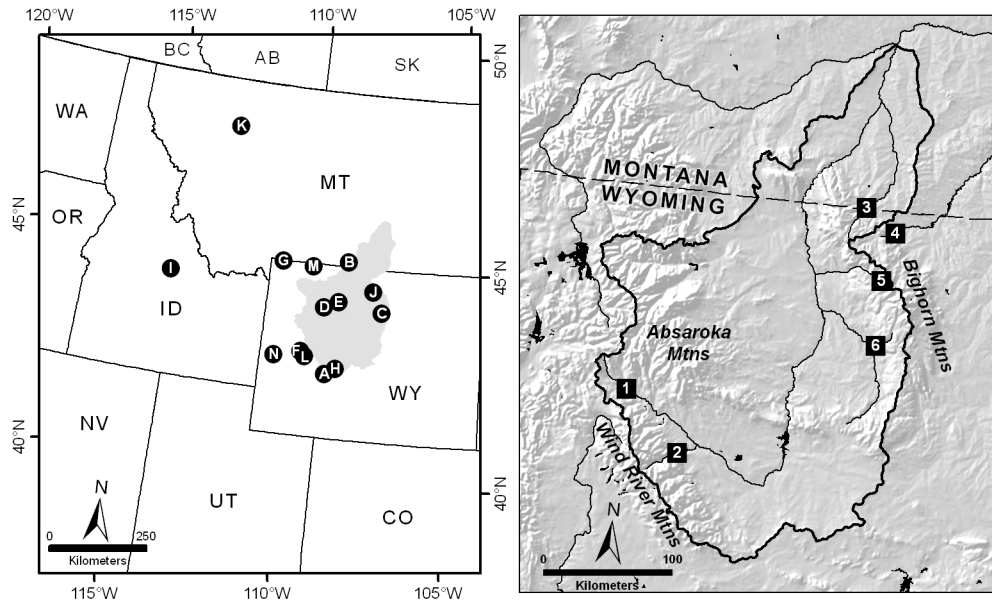
Figure 1. Map of Bighorn Basin boundary, tree-ring sites (lettered; see Table 1), and reconstructed streamflow gages (numbered; see Table 3).

reconstructed for six US Geological Survey (USGS) gages over a period reaching as far back as AD 1168 using the existing network of moisture-sensitive tree-ring chronologies from the Rocky Mountain region.  Two of these gages were previously reconstructed by Watson et al. (2009), and I provide updates to those reconstructions here.  Second, I compare statistics of the reconstructions with the 20th century gage record and evaluate the extent to which the gage record captures the natural hydrologic variability of the Bighorn Basin.  To explore the nature of long-term hydrology in the Basin I examine the magnitude, severity and duration of droughts and wet periods, and I use an event-scoring technique to compare the dry and wet events across both the reconstructed and gaged record.  Third, the reconstructed gages are distributed among the Wind River Mountains and the Bighorn Mountains bordering both the western and eastern sides of the watershed, and I examine the relative contribution of each range to long-term Bighorn

Basin hydrology.  I also evaluate the relationship between Basin hydrology and oceanic

temperature indices to explore the extent to which oceanic forcing can be used to explain

streamflow variability.  Finally, I use the extended streamflow data offered by the tree-

ring-based reconstructions to evaluate the assumptions made by the current water

management system of the Basin.  Water management within the Wyoming portion of the

Basin is guided by the Wind-Bighorn Basin Water Plan Update of 2010 (Water Plan;

WWDC, 2010).  The Water Plan uses the 1973-2008 gage record as a reference period to

identify water system vulnerabilities, assuming that this 36-year record is sufficiently

representative of long-term Basin hydrology.  I compare statistics from the

reconstructions with those of the reference period to determine whether or not the long-

term streamflow record can be used to improve the Water Plan methodology.

<center>Study Area</center>

Hydrography

The Bighorn Basin is actually composed of two distinct hydrographic basins.  The

upper portion is known as the Wind River Basin.  The Wind River begins in high

mountains near the intersection of the Washakie and Wind River Ranges on the western

border of the greater Bighorn Basin, flowing southeast then north to Boysen Reservoir

while receiving contributions from streams draining the east side of the Wind River

Range.  It exits the reservoir through Wind River Canyon in the Owl Creek Mountains

and changes name to become the Bighorn River.  In the middle and lower portions of the

Bighorn Basin, the River receives significant contributions from the Greybull and

Shoshone rivers, each of which drains the eastern slope of the Absaroka Mountains.

Nowood River, Tensleep Creek, and Shell Creek contribute runoff from the Bighorn

Mountains, which bound the east side of the Bighorn Basin. The river enters Bighorn

Lake (also known as Yellowtail Reservoir) near the town of Lovell, Wyoming. After

passing through Yellowtail Dam at Fort Smith, Montana, the Bighorn River acquires

significant flow contributions from the Little Bighorn River at Hardin, Montana. It then

follows a meandering course to its confluence with the Yellowstone River. In total, the

Wind-Bighorn River system drains approximately 59,000 km$^2$ of Wyoming and Montana,

yielding roughly 3.2 billion m$^3$ (2.6 million acre-feet) of water annually on average

(WSGS, 2011).

Climatology

The Bighorn Basin is one of the most arid basins in the western US, with the

lowest elevations receiving only 127 to 203 mm of precipitation annually (PRISM Group,

1990). This aridity is largely a result of the orographic barrier posed by the surrounding

mountain ranges that exceed 4000 m in elevation. Consequently, a rainshadow effect

exists year-round across the entire basin. Summers in the Bighorn Basin are warm, with

a July average daily temperature of 20.5°C, and the highest temperatures are typically

recorded at the confluence of the Bighorn and Yellowstone rivers near the town of

Bighorn, Montana. Typically, the coldest month is January, with an average daily

temperature of -6.8°C (NOAA, 2011).

The source of moisture to the Bighorn Basin varies with season, because it is

affected by Pacific Northwest, Southwest US, and Great Plains (central US) climate

patterns.  Generally, the Pacific Northwest region receives most of its annual precipitation in winter as moist mid-latitude cyclones track along the polar jet stream.  In the summer, the northeastern Pacific subtropical high-pressure system pushes the jet stream north of the region, limiting precipitation in the Northern Rockies ("summer-dry" in the classification of Whitlock and Bartlein, 1993).  This precipitation regime is reversed for the Southwest US, where summer continental heating drives monsoonal moisture flow northward from both the Gulf of California and the Gulf of Mexico ("summer-wet").  Under the summer-dry regime, most of the mountain ranges in the Northern Rockies receive abundant winter snowpack, including the ranges surrounding the Bighorn Basin (Mock, 1996).

With the northward movement of the jet stream in late spring/early summer, a different atmospheric circulation pattern affects the Bighorn Basin.  In addition to monsoonal moisture advection, a southerly low-level jet from the central US begins to play a significant role in Basin weather patterns.  Central US low-level jets are induced by the temperature and pressure gradient present during the spring/early summer months (April-June) between the cooler, higher-elevation western Great Plains and the warmer, lower-elevation central and southeastern US (Walters et al., 2008).  A characteristic feature of low-level jets is the advection of abundant warm, moist air from the Gulf of Mexico into the continental interior, bringing the potential for significant precipitation (Schubert et al., 1998).  With regard to the Rocky Mountain region, this flow of moisture commonly becomes entrained in the circulation of mid-latitude cyclones, bringing moisture into Colorado, Wyoming and Montana.  When such southerly and easterly

circulations encounter high mountains, orographic uplifting generates substantial rainstorms, thunderstorms, and snowstorms. These storms can bring several centimeters of rain or snow, significantly augmenting or altering the winter mountain snowpack, depending on surface temperatures. This spring pattern can comprise a significant portion of the low- to mid-elevation precipitation in the Bighorn Basin.

In the summer (July-September), precipitation comes from widely-scattered convective thunderstorms, with moisture supplied by the Pacific, Gulf of California or Gulf of Mexico via the mechanisms discussed previously (Mock, 1996). Summer thunderstorm activity tends to increase when the Bighorn Basin is under the influence of a southerly or southwesterly flow that brings subtropical moisture northward to interact with shortwave atmospheric disturbances. Such thunderstorms often produce little measureable precipitation, however, as the high temperatures and low humidity characteristic of the valley floor encourage the evaporation of rain before it reaches the ground. In terms of streamflow, the period of maximum runoff in the Bighorn Basin follows that of the Northern Rocky Mountains as a whole. Here, 65-85% of the mean annual streamflow occurs during the months of April through July (Lawrence, 1987; Lins, 1997).

Also significant to the water balance of the basin is the contribution of glaciers in the Wind River Mountains. The range contains approximately 31 km$^2$ of glaciers that drain to the Wind-Bighorn River system. Marston et al. (1989) note that a significant portion of the total Wind River flow comes from glacier meltwater. The contribution of

these glaciers is especially important during late summer and early fall, when the majority of snowpack in the Basin has melted and thunderstorm activity has decreased.

<u>Economy</u>

Agriculture, mining, and tourism are the primary economic drivers in the Bighorn Basin. Agriculture accounts for the vast majority of water use in the Basin, and although the total amount of irrigated land comprises a relatively small percentage of the total land area, the crops grown require a significant amount of water to be successful (WWDC, 2003). Hay production, typically used as livestock feed, far exceeds any other crop. The Bighorn Basin also produces roughly 87% of Wyoming's sugar beet crop. Only about 20% of Basin production is in corn, barley, and dry beans (WWDC, 2003). Livestock sales comprise about 65% of all agricultural income, and the majority of these sales are cattle. Drought in the early 2000s led to poor grazing conditions, and cattle revenues declined accordingly (WWDC, 2003).

Over the years, the Bighorn Basin, as well as all of Wyoming, has experienced repeated mining booms. Oil, natural gas, coal, uranium, bentonite, and gypsum are all important components of the Bighorn Basin mining industry, each consuming water resources (WWDC, 2003). However, the majority of consumptive water use by all mining activities is attributable to oil and natural gas extraction (WWDC, 2003). In the case of natural gas, surface or groundwater is injected into gas-bearing rock strata to release natural gas and bring it to the surface. The waste water is then reinjected into deep rock strata or stored in open-air evaporation pits (USEPA, 2011). In contrast, the extraction of coal, uranium, bentonite, and gypsum results in relatively little consumptive

use of water, with much of it being naturally non-potable (i.e., saline) and/or recycled during mineral processing (WWDC, 2003).

Most recreational uses of water are non-consumptive, but they are sensitive to water quantity and quality (Jacobs and Brosz, 1993). Activities such as fishing, boating, snowmobiling, and skiing bring millions of dollars annually into the region's economy (Gray et al., 2004). During drought years, the decrease in revenue from water-based recreation is felt quite strongly, especially by those industries that depend on Wyoming's system of reservoirs (WWDC, 2003). Bighorn Lake in particular serves as a regional recreational center, providing opportunities for warm-water fishing, boating, and swimming. Downstream of Yellowtail Dam, the Bighorn River offers quality trout fishing, with carefully-managed cold, clear streamflows year-round (Maffly, 2007). Beginning in 1999, drought conditions caused water-management challenges as various user groups reliant on the reservoir competed for limited water. By the time the drought culminated in 2007, many boat ramps were left dry, and revenue from recreation had declined significantly (Maffly, 2007). It is also important to note that activities only indirectly dependent on water, such as photography, golfing, camping, and hunting, are still sensitive to water quantity and quality. Such industries are likely susceptible to significant declines in revenue as the landscape responds to single- and multi-year drought.

Water-Resource Management

In the Bighorn Basin, layers of state laws, federal laws, interstate compacts, and court decrees influence how, where, and when water is used. Wyoming, like the western

US as a whole, adopted the prior appropriation doctrine of water rights under which the maxim "first-in-time, first-in-right" applies to water allocation during times of water stress (BLM, 2001). Water rights do not convey ownership of water, but rather allow for the priority use of water for "beneficial uses," defined as productive and non-wasteful (WWDC, 2003). Stakeholders in the Basin include a multitude of federal, state and local government agencies, as well as private landowners and businesses. The economic and political forces within the Wind River Indian Reservation also have a significant effect on water management in the whole of the Basin, since the Reservation currently holds rights to 500,000 acre-feet of water from the Wind River system (WWDC, 2003). Only about half of this water is currently put to beneficial use, but the remainder is not required to be released to downstream users during drought periods (WWDC, 2003). Combined with the heterogeneous distribution of state and federal parcels, fragmented ownership is perhaps the most difficult water management challenge, second to water supply (WWDC, 2003). Another significant legal constraint is that of interstate water compacts between Wyoming, Montana and North Dakota. Eighty percent of Wind/Bighorn River system flow is apportioned to Wyoming and the remainder flows into Montana's Yellowstone River (WWDC, 2003). The agreement, known as the Yellowstone River Compact of 1950, is presently the subject of a legal dispute under review by the US Supreme Court. The outcome of the lawsuit may require adjustments to the way water is managed in the Basin, making water management during droughts even more challenging.

## 2. BACKGROUND INFORMATION

### Tree-Rings as Hydrological Proxies

In this section, I discuss the need for accurate streamflow information and the various ways in which streamflow records are extended to capture a wider range of hydrologic variability. I review the use of tree-rings as a proxy for long-term streamflow information, including the physical relationship between tree-growth and runoff that permits robust reconstruction modeling.

Water-resource planning and infrastructure design require the best possible estimates of extreme streamflow conditions. The duration and magnitude of extremely low flow periods are of particular interest to, for example, irrigation-system managers considering whether or not to construct a new reservoir (Loáiciga, 2005). A common problem faced by water resource managers is the limited availability of instrumental streamflow data, especially in the western US where gage records are typically less than 60 years long (Woodhouse, 2004). To address the issue of short streamflow records, both deterministic and stochastic streamflow generation models are commonly used to extend gage records or to fill in missing data (Bonin and Burn, 2005). Deterministic models use the physical and hydrological characteristics of a watershed to estimate streamflow from instrumental meteorological data, typically precipitation and temperature. This method takes advantage of the fact that meteorological records are usually longer than streamflow records. Stochastic techniques include regional regression analysis and streamflow synthesis by leveraging the statistical properties of available gage data, or by cross

correlation with other nearby flow series of longer duration (Bonin and Burn, 2005). However, such synthesized records are still only as long as the 20th century instrumental record, limiting their usefulness in understanding hydroclimatic variability over long timescales.

Tree-rings provide a method of extending streamflow data hundreds of years beyond the gage period of record (Cook and Jacoby, 1983; Woodhouse, 2001; Jain et al., 2002; Case and MacDonald, 2003; Graumlich et al., 2003; Gedalof et al., 2004; Gray et al., 2004; Knight et al., 2004; Carson and Munroe, 2005; Timilsena et al., 2007; Watson et al., 2009). Essentially, tree-ring reconstructions of streamflow utilize a stochastic modeling approach in which the period of common record between a gage and nearby tree-ring chronologies (rather than another gage) is used to define a statistical relationship that permits extension of shorter gage data to the length of the longer tree-ring data (Fritts, 1976). The discrete annual growth of trees is used as a proxy for streamflow because several of the environmental factors that influence tree growth also affect streamflow, especially precipitation and evapotranspiration (Fritts, 1976; Meko et al., 1995). Careful site selection minimizes the effects of non-climatic factors on tree growth, such as insect infestation, timber harvesting, and fire (Cook and Kairiukstis, 1990). Typically, the best precipitation response has been found at warm, sunny sites located along the lower forest border, where soils are rocky and well-drained, thereby making soil moisture the predominant limiting factor to tree growth (Fritts, 1976). Once a site containing trees that show strong variation in year-to-year growth (i.e., high climate sensitivity) is located, as many trees as possible are sampled to help mitigate non-climatic

growth anomalies.  The shared signal from all trees sampled at the same site is known as a chronology.

The mechanism by which precipitation drives tree growth is not well-defined, but the direction and magnitude of the relationship is fairly predictable for certain tree species (Fritts, 1976).  In moisture-sensitive trees, low soil moisture in the root zone, as well as high evaporative demand of the atmosphere, creates low internal water potential and results in low cambial growth (Fritts, 1976).  In the western US, tree response to precipitation is not limited to the season of active cambial growth.  Many studies have shown that tree-ring series from this region are significantly correlated with precipitation during the cool-season months prior to the start of annual growth (Meko et al., 1995; Woodhouse, 2001; Graumlich et al., 2003; Woodhouse and Lukas, 2006b; Gray et al., 2007; Pederson et al., 2011).  Soil moisture is typically recharged during winter snowfall and spring snowmelt, providing water for tree growth.  The protracted melt of snowpack often extends the period of moisture availability and attendant tree-growth well into summer (Meko et al., 1995).  Therefore, the growth series of trees and data from precipitation and streamflow gages are often very highly correlated, and dendrohydrological studies exploit this relationship to estimate pre-instrumental hydrology.

## Statistical Techniques in Dendrohydrology

In this section, I provide detailed background information on the standard statistical procedures used to develop tree-ring chronologies and to create streamflow

reconstruction models.  As part of this study, I developed two new chronologies using the standard techniques outlined in this section.  However, neither were ultimately used to reconstruct Bighorn Basin streamflow.  All of the chronologies used by this study were collected and processed by other researchers, and I discuss those techniques here.  This discussion includes the detrending of tree-ring data, screening of calibration (gage) data, the treatment of autocorrelation, screening of tree-ring chronologies, and multiple-linear regression procedures.

The first step in the treatment of raw tree-ring width data is detrending (Cook and Kairiukstis, 1990).  For typical drought-sensitive trees, growth generally decreases with age after completion of the more rapid juvenile growth period.  The effects of both age and geometry on ring width are non-climatic features and must be removed statistically, while minimizing the loss of climatic information (Fritts, 1976).  A straight line with negative slope or negative exponential curve was applied to the raw series of the chronologies used by this study, but other detrending equations are available and their applications are dependent on study objectives and the site characteristics (Fritts, 1976).  Common to all reconstruction efforts is the need to evaluate both the tree-ring data and the gage data of interest for statistical rigor.  These steps identify data-quality issues at the outset and help avoid conditions that would violate the assumptions associated with multivariate analysis and linear regression typically used in climate reconstruction (Bonin and Burn, 2005).  The conditions of highest concern are those of non-normality, non-stationarity, and autocorrelation (Bonin and Burn, 2005).  For nearly all modeling procedures used in climate reconstruction, including auto-regressive moving average

(ARMA) and linear regression, normally-distributed error terms are required (Meko et al., 1995). Normality tests, including the Anderson-Darling test or the Kolmogorov-Smirnov test, were used to determine whether the data series approximated a normal probability distribution. To detect non-stationarity (i.e., shifts in the mean or variance over time), a variety of graphical exploratory data analyses were used, including box, run-sequence, and stem-and-leaf plots (Weisberg, 1985). Severely non-normal or non-stationary datasets would typically be transformed prior to reconstruction model development. Autocorrelation (i.e., correlation between successive values in a time series) in both tree-ring and streamflow data arise from the interannual carryover effects of precipitation in both tree physiology and watershed hydrology (Fritts, 1976). The tree-ring chronologies were developed in two forms, one retaining the natural autocorrelation (known as the standard chronology) and the other with the autocorrelation removed via a prewhitening process (the residual chronology; Cook and Kairiukstis, 1990). The standard versions of all chronologies were used by this study. A prewhitened version of any dataset is created by fitting an ARMA model to the time series, then using the non-autocorrelated residuals to move forward with analysis (Bonin and Burn, 2005). While some researchers elect to remove the autocorrelation from the tree-ring data and/or the streamflow data, doing so may also remove a portion of the desired climate signal (Meko et al., 1995).

Generally, before reconstruction modeling begins, potential predictor chronologies are screened for correlation with overlapping climatological data (including precipitation and temperature), as well as streamflow data (Bonin and Burn, 2005).

These instrumental datasets are usually screened for gaps or other anomalies that may be caused by measurement error, and much of this work has already been completed for the USGS gage network (Easterling and Peterson, 1995). Preferably, the period of overlap extends several decades (Gray, pers. comm., 2010). Best-subsets or stepwise multiple-linear regression (MLR), as well as principal components regression (PCR), procedures are often used to develop the relationship between a single dependent variable (here, streamflow), and several independent variables (tree-ring chronologies; Meko et al., 1995). Stepwise and best-subsets regression procedures attempt to find the simplest model possible while achieving the highest percentage of streamflow variance explained by iteratively adding and subtracting chronologies as necessary (Meko et al., 1995; Bonin and Burn, 2005). This process minimizes the effects of multicollinearity and prevents overfitting, conditions that reduce the ability of the model to predict streamflow values outside of the range of calibration values (Weisberg, 1985). Model quality is typically assessed via $R^2$, Mallows' Cp (Maidment, 1993), Variance Inflation Factor (Haan, 2001), and the Durbin-Watson statistic (Draper and Smith, 1998). Model validation is typically performed using a leave-one-out Prediction Sum of Squares (PRESS) test (Maidment, 1993). Each of these quality and validation measures was used in streamflow reconstruction modeling for the Bighorn Basin. Because the number of trees typically decreases towards the beginning of each chronology, reconstructions are usually truncated to begin at the year in which the sample depth drops below a certain level (typically 85%; see Methods section for discussion) to avoid problems with noise amplification (Wigley et al., 1984).

## History of Dendrohydrology

This section reviews the application of tree-rings to hydrologic reconstructions in the southwestern US and in and around the Bighorn Basin. The first North American scientist to be credited with formally studying the relationship between tree-rings and hydrology is A. E. Douglass, an astronomer investigating the relationship between sunspots and rainfall in the southwestern US (Bradley, 1999). Since Douglass' founding of the Laboratory of Tree-Ring Research at the University of Arizona in 1937, many researchers have developed techniques for using this proxy as an indicator of pre-instrumental hydrology. In the Colorado River Basin, Stockton and Jacoby (1976) calibrated 17 tree-ring width chronologies to the gage record at Lees Ferry, Arizona during the period 1896 to 1960. This work used stepwise multiple linear regression to reconstruct flow at Lees Ferry back to 1564 using ring widths as input. Several decades later, Woodhouse et al. (2006) expanded on this study, introducing a network of new tree-ring chronologies and a longer instrumental record for calibration. Their analysis revealed an increased long-term mean annual flow volume as well as reduced drought magnitude than the Stockton and Jacoby (1976) reconstruction. The recent findings may have resulted from the use of different predictor chronologies as well as a new statistical reconstruction methodology for the treatment of autocorrelation in the ring-width-index time series (Woodhouse et al., 2006). Elsewhere in the western US, successful hydrological reconstructions have been completed for the Columbia (Gedalof et al., 2004), Upper Yellowstone (Graumlich et al., 2003), Sacramento (Meko et al., 2001), and Snake (Wise, 2010) rivers. Watson et al. (2009) generated reconstructions for three

streamflow gages in the eastern Wind River Mountains, two of which are updated by this study.  Also in the Bighorn Basin, Gray et al. (2004) used existing Northern Rockies tree-ring data to examine long-term variability in precipitation.  My reconstructions of Bighorn Basin streamflow use many of the same techniques and tree-ring chronologies employed by these Northern Rockies studies.

# 3. DATA AND METHODS

Fifty-seven tree-ring chronologies from across the Northern Rocky Mountains were evaluated for use in Bighorn Basin streamflow reconstructions. Of this group, 26 were collected from Douglas-fir (*Pseudotsuga menziesii*), 18 from limber pine (*Pinus flexilis*), 11 from subalpine larch (*Larix lyallii*), one from ponderosa pine (*Pinus ponderosa*), and one from Engelmann spruce (*Picea engelmannii*). Each chronology was developed using standard processing methods (Fritts, 1976; Cook and Kairiukstis, 1990), and the datasets were obtained from either the International Tree Ring Data Bank or directly from the primary researchers. As noted previously, I collected and developed an additional Douglas-fir chronology in the Crazy Mountains (MT), and I developed a previously-collected Douglas-fir chronology from the Beartooth Range (MT), but neither was significantly correlated with streamflow data in the Bighorn Basin nor considered in the streamflow reconstructions (see Appendices J and K).

The pool of fifty-seven chronologies was reduced via correlation analysis with overlapping gage data to eliminate those that showed no relationship with Bighorn Basin streamflow (see following section for gage information, and Appendix A for correlation results). The standard (i.e., serial persistence retained) versions of the chronologies were used since the streamflow data contained a certain amount of autocorrelation caused by interannual persistence in the hydrological system (see Table 3). Only chronologies with strong Pearson correlations ($p<0.05$) with the gage data were allowed into the streamflow predictor pool. This process reduced the original pool from 57 to 33. To have been considered as logical predictors for streamflow reconstructions, chronologies must have

also shown significant relationships with meteorological station or climate division

precipitation, temperature, or PDSI over some part of the year.  The residual versions of

annual ring-width indices from the pool of 33 tree-ring chronologies were compared with

instrumental precipitation and temperature records via correlation analysis.  Growth data

and climate were compared at monthly, seasonal (December-February, March-May,

June-August, September-November) and water-year temporal scales during the period of

record for which the climate data were available.  I compared tree growth with individual

meteorological station data from the US Historical Climatology Network (HCN;

available at http://cdiac.ornl.gov/epubs/ndp/ushcn/access.html).  All data in the HCN

have been adjusted for measurement and location biases, and missing records have been

estimated using nearby meteorological stations (Easterling and Peterson, 1995).  I also

compared the tree-ring indices with climate division data for Wyoming, Montana and

Idaho, taken from the Desert Research Institute's WestMap database (DRI; available at

http://cefa.dri.edu/Westmap/).  Climate divisions are designed to roughly follow the

boundaries of major watersheds, making them particularly useful for streamflow

modeling.  For each climate division, data from meteorological stations were combined to

produce temperature and precipitation averages (Guttman and Quayle, 1996), reducing

the spatial biases accompanying station-level data.  Each tree-ring chronology was

compared with the nearest HCN stations and climate divisions.  Chronologies were also

compared with the nearest Palmer Drought Severity Index (PDSI) grid point (Palmer,

1965; Alley, 1984; Cook, et al., 1999).  For all comparisons, climate variables lagged by

one year ($t$-1) were also examined to check for delayed tree-growth response.  All 33

chronologies showed a significant (p<0.05) Pearson correlation with precipitation,

temperature, or PDSI (see Appendix B).  All chronologies are available for download

from the online International Tree Ring Data Bank (ITRDB) or from Gregory Pederson at

the USGS.

## Streamflow Data

Fifteen streamflow measuring stations in and adjacent to the Bighorn Basin were

identified from USGS gages in the Hydro-Climatic Data Network (HCDN) (Slack et al.,

1993).  Streamflow gages included in the HCDN have been found to be sufficiently

unaffected by anthropogenic flow alterations and thus suitable for long-term climate

analysis.  Additional candidate gages were selected using expert knowledge at the

Wyoming Water Resources Data Center (Gray, pers. comm., 2010).  I also chose to

examine several long-record gages located just outside of the Bighorn watershed in order

to increase my chances of getting successful reconstructions.  These gages are located in

the surrounding mountains and thus excellent proxies for Bighorn Basin hydroclimatic

variability (see Figure 1).  Daily streamflow data were obtained for the selected gages

from the USGS National Water Information System (http://waterdata.usgs.gov).

Candidate gages were then screened for data length and quality (i.e., recording errors,

estimated versus actual flow values, etc.).  All selected gages had a minimum length of

41 years of record, except for Tensleep Creek (USGS #6271000).  I infilled and extended

this record from 29 discontinuous years to 49 continuous years via regression analysis

with nearby gage data (Hirsch, 1979; see Appendix C).  Based on the Kolmogorov-

Smirnov test, all streamflow datasets were essentially normally distributed, containing

only slightly long tails due to extreme flow events. Gages that did not meet the requisite

length and quality thresholds were removed from further consideration. From the

original set of 15 gages, nine were deemed acceptable for reconstruction modeling with

the tree-ring data. It is important to note that streamflow data collected during the early

years of the USGS gage program were probably less accurate than more recent data. The

introduction of Acoustic Doppler Current Profilers (ADCP) to calibrate gages in the

1990s has resulted in better discharge measurements, especially during floods and low-

flow periods (Hirsch and Costa, 2004). This change in measurement accuracy has the

potential to introduce unquantifiable errors into regression modeling processes, especially

those that use pre-ADCP gage data summarized by minute, hour, or day. Such errors do

not affect my reconstruction models significantly, because gage data were summarized on

an annual basis prior to modeling.

## Streamflow-Growth Calibration Models

As described previously, the initial screening process yielded 33 tree-ring

chronologies that showed strong correlations with both climatic data and streamflow, as

well as nine streamflow gage records of suitable length and quality for reconstruction.

Forward and backward stepwise multiple-linear regression (Weisberg, 1985) was used to

create each reconstruction model. Each potential predictor chronology was entered into

the regression model in order of its streamflow variance explained. Each chronology was

required to have a $p$ value $\leq 0.05$ for entry and $p \leq 0.10$ for retention in the model.

During the modeling process, the pool of 33 potential predictor chronologies was reduced to 14 (Table 1).

Table 1. Descriptive information for tree-ring chronologies used in this study.

| Map ID[1] | Chronology | Species | Collected By | Elevation (m) | Lat | Long | Years (AD) | Year SSS >0.85 | Lag-1 ACF[2] |
|---|---|---|---|---|---|---|---|---|---|
| A | Anderson Ridge Rim, WY | *Pseudotsuga menziesii* | S. Gray, G. Pederson, T. Watson, A. Barnett | 2555 | 42° 29' 24" | 108° 55' 48" | 1519-2006 | 1615 | 0.52 |
| B | Bear Canyon, MT | *Pinus flexilis* | S. Gray | 2100 | 45° 06' 36" | 108° 30' 36" | 369-1998 | 870 | 0.82 |
| L | Boulder Lake, WY | *Pseudotsuga menziesii* | S. Gray, G. Pederson, T. Watson, A. Barnett | 2256 | 42° 51' 00" | 109° 37' 48" | 1576-2006 | 1672 | 0.53 |
| M | Clarks Fork Yellowstone, WY | *Pseudotsuga menziesii* | L. Waggonner, L. Graumlich | 2591 | 44° 55' 52" | 109° 38' 31" | 1484-1999 | 1477 | 0.4 |
| C | Cooks Canyon, WY | *Pinus ponderosa* | S. Gray | 1560 | 44° 00' 36" | 107° 17' 24" | 1392-1998 | 1450 | 0.57 |
| E | Dead Indian, WY | *Pseudotsuga menziesii* | C. Ferguson, D. Despain | 1474 | 44° 10' 48" | 108° 42' 36" | 1194-2000 | 1580 | 0.58 |
| D | Dicks Creek Ridge, WY | *Pseudotsuga menziesii* | S. Gray, G. Pederson, T. Watson, A. Barnett | 2639 | 44° 01' 37" | 109° 10' 16" | 1441-2007 | 1494 | 0.54 |
| F | Fremont Lake, WY | *Pseudotsuga menziesii* | S. Gray, G. Pederson, T. Watson, A. Barnett | 2430 | 42° 57' 36" | 109° 46' 12" | 1507-2006 | 1578 | 0.54 |
| G | Mount Everts, WY | *Pseudotsuga menziesii* | L. Graumlich, L. Waggoner, J. King, E. Ferguson | 2179 | 44° 58' 48" | 110° 39' 36" | 1168-1999 | 1240 | 0.44 |
| N | McDougal Pass, WY | *Pinus flexilis* | P. Brown, C. Woodhouse | 2743 | 42° 47' 60" | 110° 35' 60" | 870-1998 | 1485 | 0.54 |
| H | Red Canyon Unit, WY | *Pinus flexilis* | S. Gray, G. Pederson, T. Watson, A. Barnett | 1990 | 42° 37' 48" | 108° 37' 12" | 1600-2006 | 1613 | 0.45 |
| I | Salmon River Valley, ID | *Pseudotsuga menziesii* | resampled, J. Littell; original, F. Biondi | 1700 | 44° 24' 36" | 114° 15' 00" | 1135-1996 | 1350 | 0.54 |
| J | Trapper Canyon, WY | *Pseudotsuga menziesii* | S. Gray | 2103 | 44° 28' 59" | 107° 37' 01" | 1250-1998 | 1250 | 0.51 |
| K | Teton River Valley, MT | *Pinus flexilis* | L. Graumlich, L. Waggoner, C. Caruso, B. Peters | 1678 | 47° 55' 01" | 112° 43' 59" | 783-2000 | 989 | 0.45 |

[1]Corresponds with chronologies in Figure 1.

[2]Lag-1 ACF is the autocorrelation function value of the tree-ring series at a lag of 1 year.

Table 2. Predominant climate responses for tree-ring chronologies used in this study.  See Appendix B for complete tables of chronology-climate correlations.

| Map ID[1] | Chronology | Climate Variable | Pearson's R[2] |
|---|---|---|---|
| A | Anderson Ridge Rim, WY | June Total Precip | 0.44 |
| B | Bear Canyon, MT | March-April-May Total Precip | 0.43 |
| L | Boulder Lake, WY | Water Year Total Precip | 0.56 |
| M | Clarks Fork Yellowstone, WY | June Total Precip | 0.38 |
| C | Cooks Canyon, WY | Water Year Total Precip | 0.42 |
| E | Dead Indian, WY | Water Year Total Precip | 0.33 |
| D | Dicks Creek Ridge, WY | July Total Precip | 0.40 |
| F | Fremont Lake, WY | Water Year Total Precip | 0.48 |
| G | Mount Everts, WY | Water Year Total Precip | 0.47 |
| N | McDougal Pass, WY | June Total Precip | 0.33 |
| H | Red Canyon Unit, WY | June Total Precip | 0.34 |
| I | Salmon River Valley, ID | Water Year Total Precip | 0.46 |
| J | Trapper Canyon, WY | Calendar Year Total Precip | 0.43 |
| K | Teton River Valley, MT | April Maximum Temp | -0.31 |

[1]Corresponds with chronologies in Figure 1.

[2]All correlations are significant at the 95% confidence level.

The residuals for the regression models were reviewed graphically for non-normality and trend, conditions that might indicate the need for data transformation. To protect against model overfitting, the entry of more predictors was stopped when the root-mean-square error (Weisberg, 1985) stopped improving. Additionally, the Mallows' Cp statistic (Weisberg, 1985; Maidment, 1993) was evaluated at each step. Multicollinearity of the predictors was evaluated using the variance inflation factor (VIF; (Haan, 2001)), and the Durbin-Watson statistic (Draper and Smith, 1998) was used to check for autocorrelation within the residuals. The fit and strength of each model were evaluated using $R^2$ and adjusted $R^2$, and leave-one-out cross-validation was performed using the prediction sum of squares test (PRESS; Weisberg, 1985; Maidment, 1993). The PRESS procedure is a leave-one-out regression method that reruns the regression multiple times, each time leaving out one value from the calibration (gage) dataset. The prediction of the left-out value is then compared to its actual value. Therefore, the PRESS $R^2$ provides an indication of the ability of the final regression model to predict streamflow values that were not included in the calibration data set. Each final reconstruction represented a composite of shorter models, each of which was optimized for quality and length. The more recent segments of each reconstruction were composed of multiple overlapping tree-ring chronologies and had a high level of streamflow variance explained. The older segments had chronologies of shorter duration removed and were characterized by lower streamflow variance explained. The goal was to create reconstructions of the longest possible length while maintaining acceptable model quality throughout. For quality control purposes, I assessed the fidelity through time of each chronology via the

subsample signal strength (SSS) criterion (Wigley et al., 1984). Each segment of each reconstruction was truncated at the year in which the SSS of the longest chronology dropped below 0.85 (as recommended by Wigley et al., 1984), indicating that less than 85% of a common hydroclimatic signal was retained among the trees in that chronology due to decreased sample depth. Before combining each model into a final reconstruction, the mean and variance of each were scaled to match those of the most recent model. The use of Principal Component Regression (PCR) to create the reconstructions was also investigated. In this approach, a Principal Components Analysis was run on the correlation matrix of those chronologies having significant correlation with the modeled gage. Only those components showing significant correlation with the gage data were retained in the final predictor pool. The predictor pool was thus reduced to express orthogonal modes of common variation in the tree-ring data. In this study, however, the PCR-based reconstructions performed poorly compared to stepwise-regression versions (e.g., $R^2$ values > 0.1 lower), so subsequent analyses were limited to the stepwise-regression-generated reconstructions.

<u>Analysis of Streamflow Reconstructions</u>

For each gage, separate statistical summaries were performed for the reconstruction and the complete gage record. The gage statistics were compared to their equivalent reconstruction statistics to determine the extent to which the gage record represents the statistical structure of long-term hydrology in the Bighorn Basin. Single-year departures from average streamflow were also calculated. Multi-year to decadal

streamflow variability was explored quantitatively by analyzing the duration and severity of dry and wet runs in the reconstructions. Following the methodology described by Dracup et al. (1980), a run is defined as two or more consecutive years above or below the mean gage flow value. For each reconstruction, streamflow departures from the gage mean were calculated and runs of years above and below this threshold were grouped. Each run was evaluated for duration, deficit/surplus (cumulative departure), and intensity (deficit/surplus divided by duration). Then, the effective severity of each event was normalized by assigning each of them a single score (Biondi et al., 2002). Treating wet and dry events separately, all cumulative departure values and intensity values were ranked. The event score was then calculated as the sum of the cumulative departure rank and the intensity rank. Following scoring, event scores were compared within and between the reconstructed and gaged record.

<center>Relationship to Oceanic Climate Variability</center>

To explore possible relationships between oceanic climate variability and Bighorn Basin hydrology, reconstructed water-year streamflows were compared with the Nino-3.4 Southern Oscillation Index from the National Center for Atmospheric Research (NCAR; available at http://www.cgd.ucar.edu/cas/ENSO/enso.html) and the PDO index (Mantua et al., 1997; available at http://jisao.washington.edu/pdo/PDO.latest). Streamflow reconstructions were standardized into z-scores, then grouped and averaged by mountain range (Wind River Range and the Bighorn Range), such that each range was represented by a single streamflow series. Each series was correlated with monthly, annual, and

seasonal averages of the PDO and ENSO index. The analysis was performed over the

period from 1900 to 1996, representing the timeframe of complete overlap between the

oceanic climate indices and the streamflow reconstructions.

<u>Comparison with Wind-Bighorn Basin Water Plan Statistics</u>

The 20th and 80th percentile values are presently used to classify 1973-2008

annual flows into dry ($\leq$ 20th percentile), average, and wet ($\geq$ 80th percentile) categories

for water planning purposes in the 2010 Wind-Bighorn Basin Water Plan Update

(WWDC, 2010). The Water Plan is a document that calculates threshold values for a

representative subset of Basin gages and uses them as inputs for scenario modeling. Even

though I did not reconstruct the same streamflow gages used by the Water Plan, the

distribution of the reconstructed gages across the high elevations of the Basin suggests

that they are sufficiently representative of Basin-wide hydrology and thus comparable to

the Water Plan gage network. I evaluated the assumption that the 1973-2008 reference

period was representative of long-term Basin conditions by calculating the percentile

values for this 36-year period for my six streamflow gage records. I then compared the

36-year gage percentiles with the same statistics for the respective long-term

reconstructions.

## 4. RESULTS

Streamflow Reconstructions

Of the nine streamflow gages for which reconstructions were attempted, three
(Clear Creek near Buffalo, WY; Clarks Fork of the Yellowstone River near Belfry, MT;
and South Fork of the Shoshone River near Valley, WY) failed to meet quality thresholds
for further consideration. Although the streamflow data from each of these gages showed
significant correlations ($p<0.05$) with at least a few tree-ring chronologies, regression
models explaining more than 20 to 30 % of the streamflow variance could not be
generated. PCR-based modeling yielded similar results. Therefore, a total of six gages
were successfully reconstructed (Table 3).

The final, composite streamflow reconstructions ranged from 493 to 829 years in
length (420 to 749 years if limited to the period in which SSS is greater than 0.85; Table
4). For example, the earliest water year of the Bull Lake Creek reconstruction is AD
1447, but the chronology sample depth is limited (i.e., SSS < 0.85)  prior to AD 1580.
See Appendix D for complete reconstruction model equations.

Table 3. Descriptions of USGS streamflow gages reconstructed in this study.

| Map ID[1] | Gage Name | USGS ID | Elevation (m) | Lat | Long | Drainage Area (km$^2$) | Usable Years of Record | Mean Annual Flow (Mm$^3$) | Coefficient of Variation (CV) | Lag-1 ACF[3] |
|---|---|---|---|---|---|---|---|---|---|---|
| 1 | Wind River near Dubois, WY | 6218500 | 2191 | 43° 34' 43" | 109° 45' 33" | 601 | 47 | 147 | 28.36 | 0.24* |
| 2 | Bull Lake Creek above Bull Lake, WY | 6224000 | 1790 | 43° 10' 36" | 109° 12' 09" | 484 | 46 | 256 | 21.49 | 0.06* |
| 3 | Little Bighorn River at Wyola, MT | 6289000 | 1326 | 45° 00' 25" | 107° 36' 52" | 471 | 58 | 131 | 26.06 | 0.42 |
| 4 | Tongue River near Dayton, WY | 6298000 | 1237 | 44° 50' 58" | 107° 18' 14" | 534 | 56 | 153 | 26.11 | 0.29 |
| 5 | Shell Creek above Shell Res., WY | 6278300 | 2758 | 44° 30' 29" | 107° 24' 11" | 60 | 41 | 30 | 23.63 | 0.24* |
| 6 | Tensleep Creek near Tensleep, WY | 6271000 | 1423 | 44° 03' 28" | 107° 23' 14" | 640 | 49[2] | 118 | 17.36 | 0.15* |

[1]Corresponds with gages in Figure 1.
[2]Gage data were extended from 29 to 49 years via regression with nearby gages. Gage decommissioned after 1992.
[3]Lag-1 ACF is the autocorrelation function value of the tree-ring series at a lag of 1 year.
*Not significant at the 95% confidence level.

Table 4. Calibration and verification statistics for the reconstruction models.

| Gage Name | Model Segment | Start Year (AD) | Year (AD) SSS >0.85* | End Year (AD) | Total Length with SSS >0.85 | Predictors Used | $R^2$ | $R^2$ (adjusted) | $R^2$ (PRESS) | SE (Mm$^3$) |
|---|---|---|---|---|---|---|---|---|---|---|
| Wind River near Dubois, WY | WIND1 | 1507 | 1580 | 1999 | 420 | 4 | 49.1 | 44.3 | 37 | 28.4 |
| Bull Lake Creek above Bull Lake, WY | BLAKE1 | 1659 | | 2000 | 421 | 3 | 61.9 | 59.2 | 54 | 33.7 |
| | BLAKE2 | 1447 | 1580 | 1658 | | 3 | 53.9 | 50.3 | 45.9 | 36.9 |
| Little Bighorn River at Wyola, MT | LTLBG1 | 1600 | | 1996 | 647 | 5 | 52.9 | 48.3 | 42 | 23.4 |
| | LTLBG2 | 1450 | | 1599 | | 4 | 40.9 | 36.5 | 29.6 | 26 |
| | LTLBG3 | 1168 | 1350 | 1449 | | 3 | 36.8 | 33.3 | 28.5 | 26.6 |
| Tongue River near Dayton, WY | TONGE1 | 1587 | | 1996 | 647 | 4 | 55.7 | 52.3 | 47.8 | 25.3 |
| | TONGE2 | 1450 | | 1586 | | 4 | 52.9 | 49.2 | 43.5 | 26.1 |
| | TONGE3 | 1168 | 1350 | 1449 | | 3 | 45.7 | 42.5 | 37.1 | 27.8 |
| Shell Creek above Shell Res., WY | SHLAB1 | 1450 | | 1998 | 749 | 3 | 55.4 | 51.8 | 46.1 | 4.5 |
| | SHLAB2 | 1250 | 1250 | 1449 | | 2 | 47.7 | 44.9 | 39.4 | 4.9 |
| Tensleep Creek near Tensleep, WY | TENSL1 | 1450 | | 1998 | 749 | 3 | 59.3 | 56.5 | 53.8 | 13.5 |
| | TENSL2 | 1250 | 1250 | 1449 | | 2 | 44.5 | 42.1 | 38.5 | 15.5 |

*Indicates the year prior to which the subsample signal strength (SSS) drops below 0.85 (see Wigley et al., 1984).

Total streamflow variance explained ($R^2$) ranged from 0.37-0.62, values that are similar to previous reconstructions in the Wind River portion of the Bighorn Basin (Watson et al., 2009), as well as other regional hydroclimatic reconstructions (Graumlich et al., 2003; Barnett et al., 2010; Wise, 2010). The PRESS $R^2$ statistic suggested that the models were skillful in predicting annual streamflow values that were not included in the calibration (i.e., gage) dataset. The reconstructions all followed a normal distribution and the Durbin-Watson statistic suggested no issues with autocorrelation in the residuals.

All of the reconstructions sufficiently captured wet and dry years in the gage record, including severe drought years (e.g., 1961 and 1989; Figure 2).

Additionally, the 1950s drought period and 1970s wet period were adequately represented by the reconstruction models. However, in several of the models the high-flow years were underestimated by the reconstruction equation. In 1964, the three northernmost Bighorn Range models failed to predict the correct sign of water-year streamflow. This inconsistency may have been caused by localized runoff anomalies that were recorded by gages in the northern portion of the Range but not elsewhere in the Basin. One successful reconstruction (Tongue River near Dayton, WY) is located outside of the Bighorn River watershed. Located on the eastern side of the Bighorn Mountain Range (see Figure 1), the Tongue River gage shows a similar hydrograph to the other three reconstructed gages on the west side of the Range that drain to the Bighorn watershed. This gage had a long period of record that was strongly correlated with regional long-lived tree-ring chronologies, and thus particularly useful for understanding the hydroclimatic history of the Bighorn Basin, as well as the Tongue Basin. The

complete reconstructions, along with their respective 20-year smoothing spline curves

and gage record mean annual flow, are plotted in Figure 3.  Appendix G includes tables

of the reconstructed streamflow values and associated confidence limits.


Figure 2. Tree-ring-based streamflow reconstructions compared with the respective gage
record.  Plot numbers refer to Figure 1 map.
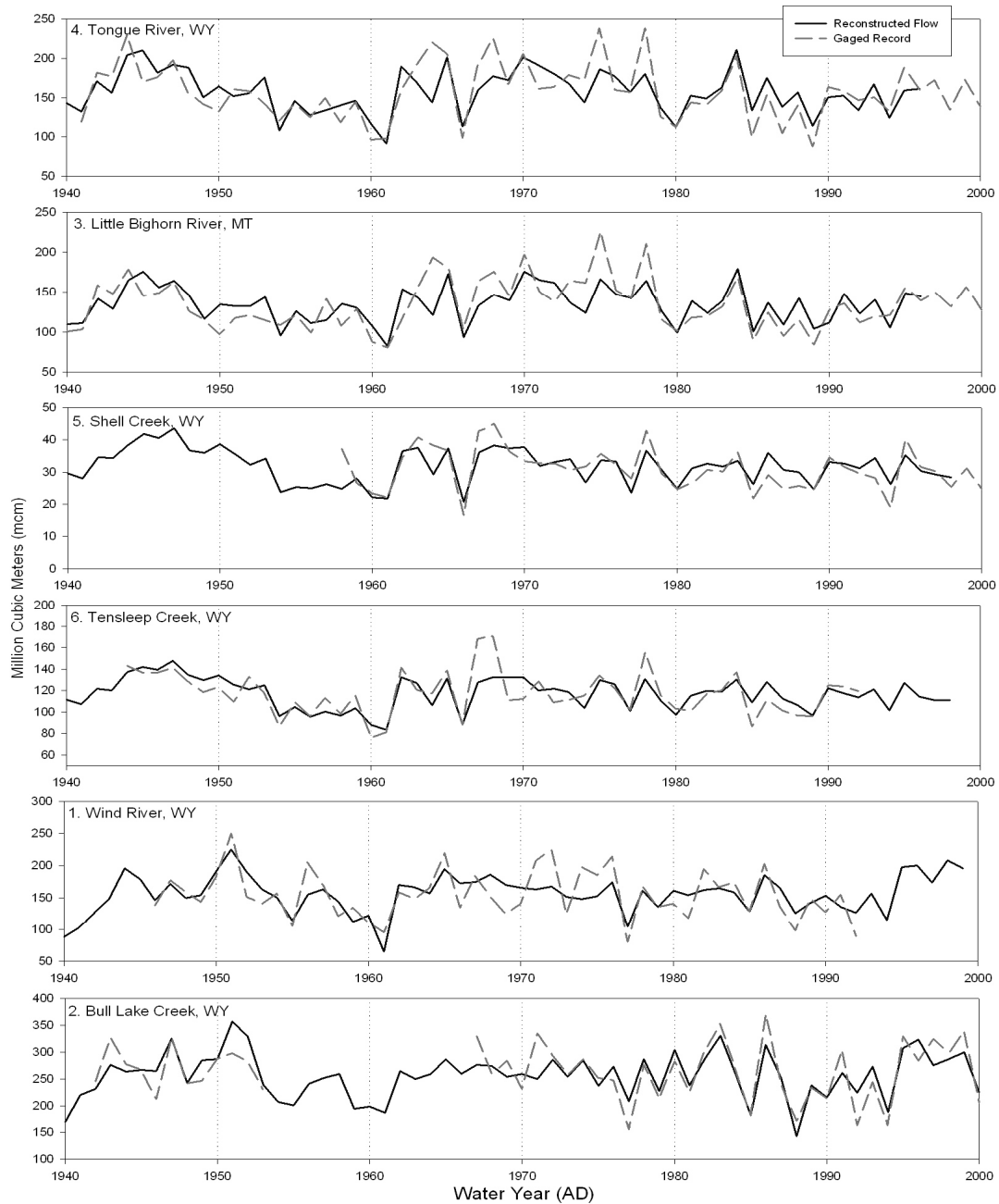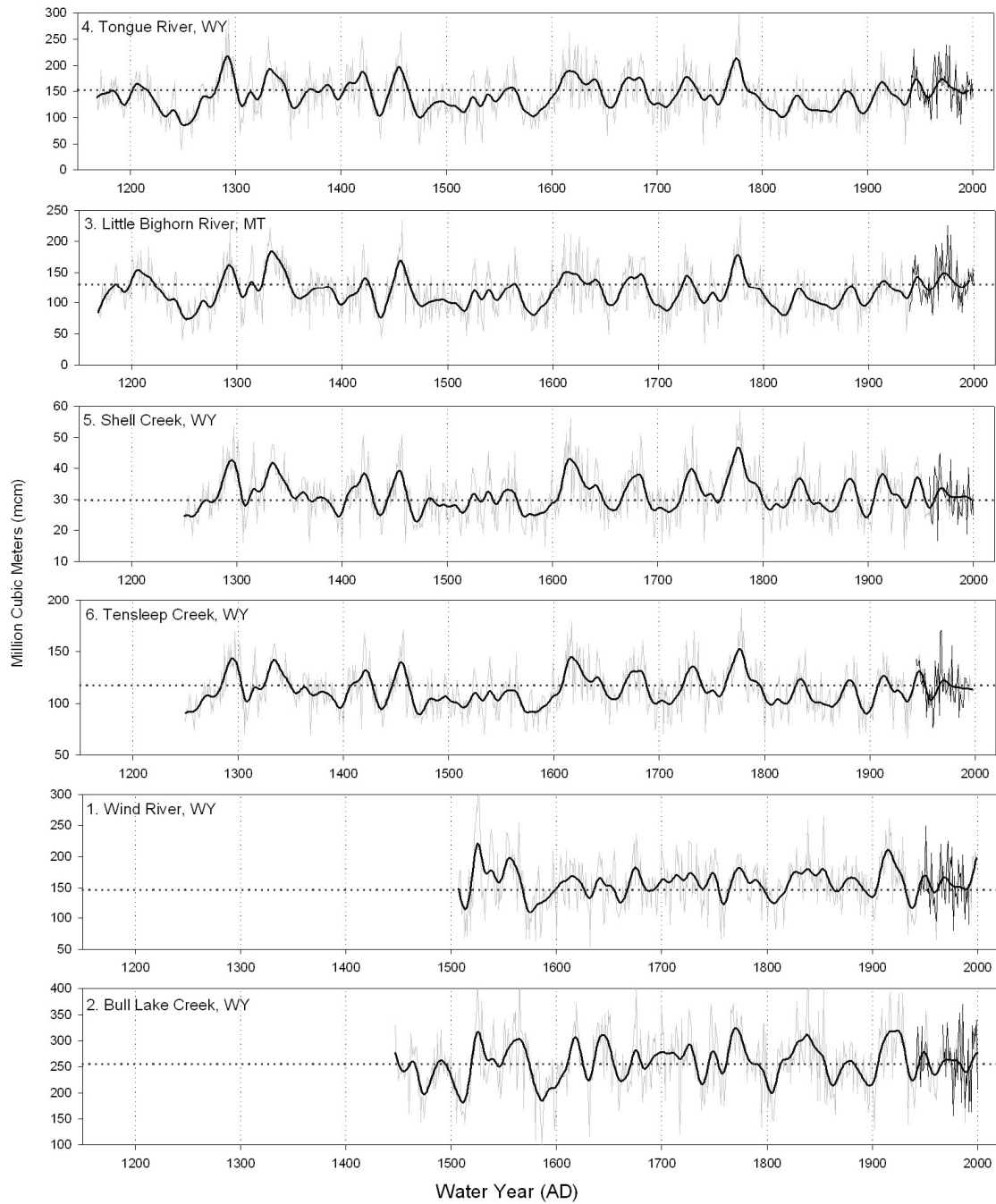
Figure 3. Tree-ring-based streamflow reconstructions (gray lines), with 20-year smoothing splines (bold black lines), gage means (horizontal dotted lines), and gage record (thin black lines). Plot numbers refer to Figure 1 map.

Preinstrumental Streamflow Variability

To compare single-year streamflow variability of the 20th century with that of the reconstructed record, I calculated a variety of summary statistics for each gage (Table 5).

For all streams, the mean water-year flows for the gage record and the reconstructed record were similar (less than 10% difference). Conversely, with the exception of Wind River (WY), the reconstructed minimum flows were substantially lower than those found in the gage record. In the case of the Little Bighorn River WY, the reconstructed minimum was 49% lower than the minimum of the gage record, a difference of 33.3 $Mm^3$. Similarly, the difference in minimum annual flows between the gage record and reconstruction for Tongue River WY was 41% less (26.4 $Mm^3$). In the case of Bull Lake Creek WY, the minimum water-year flow as recorded by the gage was 155.8 $Mm^3$, while the reconstructed minimum was 94.7 $Mm^3$, a difference of 61.1 $Mm^3$. With regard to reconstructed maximum flows, all streams showed values ranging from 7 to 30% greater than those found in the gage record. The largest relative difference (30%) was seen in Shell Creek WY, where the reconstructed maximum was 13.7 $Mm^3$ greater than that of the gage record.

Table 5. Selected water-year flow statistics for the instrumental and reconstructed record of each gage, in Mm$^3$.

| Gage Name | Complete Instrumental Record | | | | | | Reconstruction | | | | | |
|---|---|---|---|---|---|---|---|---|---|---|---|---|
| | Number of Years | Std Dev | Min | Mean | Max | CV* | Number of Years | Std Dev | Min | Mean | Max | CV* |
| Wind River near Dubois, WY | 55 | 41.7 | 49.5 | 147 | 249.9 | 28.4 | 493 | 38.5 | 54.9 | 157.7 | 318.1 | 24.4 |
| Bull Lake Creek above Bull Lake, WY | 54 | 54.9 | 155.8 | 255.5 | 370.6 | 21.5 | 554 | 55.3 | 94.7 | 257.7 | 466.9 | 21.5 |
| Little Bighorn River at Wyola, MT | 70 | 34.1 | 68 | 130.9 | 225.6 | 26.1 | 829 | 33.5 | 34.8 | 118.5 | 240.4 | 28.3 |
| Tongue River near Dayton, WY | 68 | 39.9 | 63.8 | 153 | 238.7 | 26.1 | 829 | 38.6 | 37.4 | 143 | 297.6 | 27 |
| Shell Creek above Shell Res., WY | 51 | 7 | 16 | 29.7 | 45 | 23.6 | 749 | 7.4 | 11.6 | 31.5 | 58.6 | 23.6 |
| Tensleep Creek near Tensleep, WY | 49 | 20.4 | 76.3 | 117.6 | 170.8 | 17.4 | 749 | 20.4 | 64 | 112.8 | 191.2 | 18.1 |

* Coefficient of Variation: Normalized measure of dispersion, calculated as the ratio of the standard deviation to the mean.

In addition to this increased spread in water-year flow values (i.e., lower minimums and higher maximums), the reconstructions revealed dramatic interannual variability (see Figure 3). For example, throughout the Little Bighorn reconstruction water-year streamflow fluctuations regularly exceeded 20 $Mm^3$, an amount equivalent to 15% of the long-term mean water-year flow (see Appendix E). Abrupt changes of the same relative size were seen in the neighboring Tongue River reconstruction. In terms of relative magnitude, streams with the greatest average year-to-year fluctuation in flow were the Little Bighorn (25.5 $Mm^3$) and Tongue Rivers (29.6 $Mm^3$), representing roughly 19% of their respective gage mean flows. The decline in estimated streamflow from 1617 to1618 was noteworthy for all four of the Bighorn Range gages. The quantity of water represented by this single-year decrease equals nearly 30% of the mean water-year flow for each stream. Notably, the Little Bighorn River reconstruction shows the greatest variability in year-to-year streamflow with a coefficient of variation of 28.3. For this gage, annual streamflow variations ranged from 0.05 $Mm^3$ to 120.2 $Mm^3$ (Appendix E). Single-year fluctuations approaching this magnitude have not occurred in any of the 20th century gage records.

In addition to single-year variability, I explored the nature of multi-year variability in Bighorn Basin streamflow. Researchers have used several methods to quantify the nature of drought in streamflow series, including runs analysis (Dracup et al., 1980), intervention analysis (Box and Tiao, 1975), and stochastic modeling (Biondi et al., 2002). In my study, the goal was to explore the relative differences in drought character between the pre-1900 period and the 20th century. Multi-year to decadal streamflow

variability was explored quantitatively by analyzing the duration and severity of dry and

wet runs (defined as two or more consecutive years of streamflow below the gage mean)

in the reconstructions, treating the 20th century separately. For each reconstruction,

streamflow departures from the gage mean were calculated and runs of years above and

below this threshold were grouped. As described previously, each run was evaluated for

duration, deficit/surplus (cumulative departure), and intensity (deficit/surplus divided by

duration). Then, to determine the effective severity of each run I normalized them by

assigning each of them a single score (Biondi et al., 2002). Treating wet and dry runs

separately, all cumulative departure values and intensity values were ranked. The run

score (or event score) was the sum of the cumulative departure rank and the intensity

rank. Table 6 shows the highest-scoring dry and wet events for each gage, with pre-1900

and 20th century events listed separately for comparison. Figure 3 provides visual

representations of the drought events listed in the table.

Table 6. Dry (below gage mean streamflow) and wet (above gage mean streamflow) events for each reconstruction, ordered by score. The deficit and surplus are the cumulative departure of the event from the mean (in $Mm^3$), and the intensity is the cumulative departure divided by the duration (Biondi et al., 2002). The deficit/surplus values for all events are ranked, as are the intensity values. The event score is the sum of these two ranks. The top three dry/wet events are shown for both the pre-1900 period and the 20th century. Refer to Figure 3 for visual representations of these events.

| | Dry Events | | | | | Wet Events | | | | |
|---|---|---|---|---|---|---|---|---|---|---|
| **Gage Name** | **Years (AD)** | **Duration** | **Deficit** | **Intensity** | **Score** | **Years (AD)** | **Duration** | **Surplus** | **Intensity** | **Score** |
| Wind River near Dubois, WY | 1571-1580 | 10 | -457.22 | -45.72 | 76 | 1522-1528 | 7 | 805.9 | 115.13 | 116 |
| | 1510-1516 | 7 | -306.86 | -43.84 | 73 | 1536-1541 | 6 | 376.21 | 62.70 | 110 |
| | 1584-1586 | 3 | -163.75 | -54.58 | 72 | 1549-1562 | 14 | 617.31 | 44.09 | 108 |
| | 2001-2008 | 8 | -388.9 | -48.61 | 77 | 1906-1918 | 13 | 787.95 | 60.61 | 112 |
| | 1936-1942 | 7 | -276.58 | -39.51 | 66 | 1995-1999 | 5 | 242.27 | 48.45 | 97 |
| | 1933-1934 | 2 | -93.97 | -46.99 | 62 | 1920-1929 | 10 | 353.7 | 35.37 | 92 |
| Bull Lake Creek above Bull Lake, WY | 1584-1595 | 12 | -786.23 | -65.52 | 86 | 1836-1839 | 4 | 405.53 | 101.38 | 96 |
| | 1501-1518 | 18 | -1113.78 | -61.88 | 85 | 1673-1676 | 4 | 365.51 | 91.38 | 92 |
| | 1800-1809 | 10 | -703.99 | -70.40 | 85 | 1564-1568 | 5 | 388.27 | 77.65 | 91 |
| | 2000-2004 | 5 | -307.98 | -61.60 | 73 | 1912-1918 | 7 | 501.22 | 71.60 | 89 |
| | 1900-1905 | 6 | -315.8 | -52.63 | 71 | 1920-1933 | 14 | 759.59 | 54.26 | 80 |
| | 1934-1942 | 9 | -416.38 | -46.26 | 70 | 1906-1910 | 5 | 285.92 | 57.18 | 72 |
| Little Bighorn River at Wyola, MT | 1243-1281 | 39 | -1679.7 | -43.07 | 137 | 1325-1343 | 19 | 851.84 | 44.83 | 109 |
| | 1430-1442 | 13 | -632.71 | -48.67 | 137 | 1768-1781 | 14 | 578.31 | 41.31 | 105 |
| | 1813-1831 | 19 | -771.3 | -40.59 | 130 | 1621-1625 | 5 | 215.31 | 43.06 | 103 |
| | 2000-2006 | 7 | -289.21 | -41.32 | 116 | 1944-1948 | 5 | 152.31 | 30.46 | 84 |
| | 1933-1941 | 9 | -286.18 | -31.80 | 94 | 2007-2008 | 2 | 85.03 | 42.52 | 84 |
| | 1959-1961 | 3 | -73.59 | -24.53 | 58 | 1913-1916 | 4 | 98.14 | 24.54 | 66 |

Table 6 Continued

| | | | | | | | | | | |
|---|---|---|---|---|---|---|---|---|---|---|
| Tongue River near Dayton, WY | 1243-1266 | 24 | -1415.23 | -58.97 | 124 | 1284-1299 | 16 | 823.06 | 51.44 | 137 |
| | 1432-1442 | 11 | -538.43 | -48.95 | 115 | 1452-1457 | 6 | 406.93 | 67.82 | 137 |
| | 1227-1241 | 15 | -671.85 | -44.79 | 114 | 1767-1781 | 15 | 764.92 | 50.99 | 135 |
| | 2000-2006 | 7 | -383.03 | -54.72 | 112 | 1913-1916 | 4 | 149.98 | 37.50 | 113 |
| | 1933-1941 | 9 | -332.46 | -36.94 | 91 | 1942-1948 | 7 | 231.96 | 33.14 | 108 |
| | 1922-1924 | 3 | -100.09 | -33.36 | 70 | 2007-2008 | 2 | 85.76 | 42.88 | 102 |
| Shell Creek above Shell Res., WY | 1466-1477 | 12 | -84.5 | -7.04 | 114 | 1609-1617 | 9 | 127.06 | 14.12 | 141 |
| | 1393-1401 | 9 | -60.19 | -6.69 | 108 | 1761-1783 | 23 | 270.55 | 11.76 | 140 |
| | 1800-1801 | 2 | -21.36 | -10.68 | 106 | 1286-1303 | 18 | 201.45 | 11.19 | 137 |
| | 2000-2004 | 5 | -48.23 | -9.65 | 121 | 1906-1918 | 13 | 109.86 | 8.45 | 125 |
| | 1933-1934 | 2 | -17.56 | -8.78 | 94 | 1942-1953 | 12 | 90.68 | 7.56 | 114 |
| | 1954-1961 | 8 | -40.73 | -5.09 | 91 | 1967-1973 | 7 | 40.41 | 5.77 | 94 |
| Tensleep Creek near Tensleep, WY | 1466-1479 | 14 | -394 | -28.14 | 129 | 1770-1781 | 12 | 406.28 | 33.86 | 94 |
| | 1567-1598 | 32 | -739.1 | -23.10 | 128 | 1452-1459 | 8 | 230.47 | 28.81 | 88 |
| | 1889-1906 | 18 | -438.34 | -24.35 | 128 | 1609-1617 | 9 | 259.19 | 28.80 | 88 |
| | 1954-1961 | 8 | -172.95 | -21.62 | 108 | 1942-1953 | 12 | 166.21 | 13.85 | 67 |
| | 1933-1941 | 9 | -188.14 | -20.90 | 107 | 1913-1916 | 4 | 79.27 | 19.82 | 66 |
| | 1922-1924 | 3 | -78.26 | -26.09 | 105 | 1967-1973 | 7 | 61.92 | 8.85 | 42 |

Based on the event scores, the most severe drought in the last several centuries occurred in the mid 1200s. Although only two of the six reconstructions were long enough to capture this drought, previous studies corroborate the occurrence of a persistent, widespread "megadrought" during this time period (Stahle et al., 2000; Cook, 2004; Meko et al., 2007; Barnett et al., 2010). The Tongue River and Little Bighorn River reconstructions show that the mid 1200s drought period eventually produced a combined deficit of more than 3000 $Mm^3$ for these streams, an amount equivalent to more than one-half of the present total reservoir storage capacity in the Bighorn Basin. The most severe drought captured by all of the reconstructions (except Wind River due to length) began in 1466 and lasted nearly fifteen years. All of the reconstructions captured the well-known series of 16th century droughts, the most severe of which occurred late in the century (Stahle et al., 2000). The cumulative water deficit during this period varied among the streams, ranging in volume from 5 to 10 times more than the average total annual flow. Considering just the Wind River Range reconstructions, all but one of the worst-dry events occurred in the 16th century. Similarly, the Bighorn Range streams experienced drought for most of this century.

The most severe post-1900 dry event shared among all of the streams was the recent drought that began with the 2000 water-year. Almost as severe was the 1930s "Dust Bowl" drought, which lasted nearly a decade and brought substantial water deficits to the Bighorn Basin. For all but two of the reconstructed streams, the pre-instrumental droughts outscored any of the 20th or 21st century events. Considering both the gage and the reconstructed record, the 2000s drought was the worst event for the Wind River and

Shell Creek, but only by a small margin. Furthermore, each reconstruction featured several droughts lasting ten or more years, an event that has not occurred in the 20th century, even in the 1930s. The event scores also reveal that various combinations of event duration and deficit led to drought. For example, the two most-severe droughts in the Little Bighorn River reconstruction share the same event score (137) even though one lasted 26 years longer. The 1430-1442 event was 5 $Mm^3$ more intense than the 1243-1281 event and produced a level of drought stress disproportionate to its duration. Similarly, the 2000s drought scored highly because of its severe water deficits, not because it lasted longer than previous droughts.

Anomalous wet periods also occurred in the pre-instrumental record. The strongest wet event captured by all of the reconstructions occurred in the late 18th century and was characterized by a cumulative surplus streamflow volume equal to many times the mean annual flow of each gage. For example, this event ran for fifteen years and resulted in a 715 $Mm^3$ surplus in the Tongue River reconstruction, an amount equivalent to five times the average annual flow at the Dayton, WY gage. However, this wet period preceded one of the highest-scoring droughts in the Bighorn Basin reconstruction history. For the Tongue River, this early 19th century drought lasted twelve years and created a deficit of 520 $Mm^3$, effectively negating 73% of the previous surplus. Similar to the dry event results, 20th century wet event scores did not meet or exceed those of pre-20th century wet events.

As evidenced by the late 18th/early 19th century switch between wet and dry streamflow conditions, the reconstructed record shows abrupt, irregular shifts in Bighorn

Basin hydrology. The 20th century instrumental record includes similar shifts. The 1930s drought was preceded by nearly two decades of above-average streamflow for all study gages, and the 1950s drought was preceded by a multi-year wet period. Similarly, the recent drought in the Northern Rocky Mountains since 1999 was preceded by generally wet periods in the late 1980s and early 1990s. When viewed in the context of the last 800 years, 20th century wet periods have few analogs in the reconstructed record, whereas the 20th century droughts are matched or exceeded many times. See Appendix F for complete drought and wet event tables for each reconstruction.

<u>Spatial Differences in Streamflow</u>

The streamflow reconstructions were highly correlated over the past four centuries, especially among the gages located in the same mountain range (see Table 7, Figure 1 and Figure 3). A portion of the shared variance among the reconstructions was likely due to shared tree-ring chronologies in the regression models. In addition, the close proximity of the gages argue for similar hydrologic responses.

Table 7. Correlations between streamflow reconstructions. TONGE=Tongue River, LTLBG=Little Bighorn River, SHLAB=Shell Creek, TENSL=Tensleep Creek, WINDB=Wind River, BLAKE=Bull Lake Creek.

|  |  | TONGE | LTLBG | SHLAB | TENSL | WINDB |
|---|---|---|---|---|---|---|
| **Bighorn Range** | **LTLBG** | 0.94 |  |  |  |  |
|  | **SHLAB** | 0.82 | 0.80 |  |  |  |
|  | **TENSL** | 0.86 | 0.83 | 0.98 |  |  |
| **Wind River Range** | **WINDB** | 0.48 | 0.47 | 0.57 | 0.51 |  |
|  | **BLAKE** | 0.35 | 0.33 | 0.44 | 0.41 | 0.65 |

Dry (wet) years in one reconstruction were typically expressed as dry (wet) years in the other reconstructions. However, when grouped by mountain range (Wind River Range and the Bighorn Range), the reconstructions showed many years in which average flow from one range was coupled with below-average flow from the other. To evaluate the synchronicity in streamflow between the mountain ranges, the two Wind River Range reconstructions and the four Bighorn Range reconstructions were summed for each of the 490 years in which all six reconstructions overlapped (1507-1996). Using thresholds defined by the Water Plan (WWDC, 2010), each year was classified as dry, average, or wet. Figure 4 summarized the number of years that fall into each classification for both the full 490-year comparison period (4A) and the 20$^{th}$ century (4B).



Figure 4. Matrix of 490 water-years of overlapping streamflow reconstructions, combined by mountain range and categorized by hydrologic conditions. Dry ($\leq$ 20th percentile), average, and wet ($\geq$ 80th percentile) category definitions taken from Wind-Bighorn Basin Water Plan Update (WWDC, 2010). Figure 4A is for the entire 490-year comparison period; Figure 4B is for the 20$^{th}$ century only.

Across the full comparison period, there were ten years (2% of those compared; see Appendix H) in which anomalously wet conditions in one range were offset by severe

drought in the other.  Such years were randomly distributed across the comparison period, with no more than two occurring in succession.  More common (81% of the years compared) were years in which streamflow in one range was very low or very high while streamflow in the other fell somewhere between these extremes.  Evaluating just the 20$^{th}$ century, the classification revealed no years when streamflow was extremely different between the two mountain ranges, and few very wet or very dry years, as discussed previously.  Rather, approximately half of the years showed the same classification between the ranges and the other half showed various combinations of very low/high flow in one range and average flow in the other.  To examine synchronicity on longer timescales, I calculated z-scores for all of the reconstructions, averaged them by mountain range, and applied a 10-year spline smoothing algorithm to the two series (Figure 5).  The plots indicate that streamflow variability was quite similar between the two mountain ranges at the decadal timescale, with differences in magnitude rather than sign.  This finding suggests that, despite the occasional significant difference in single-year runoff between the two ranges, each showed essentially the same response during multi-year wet and dry periods.
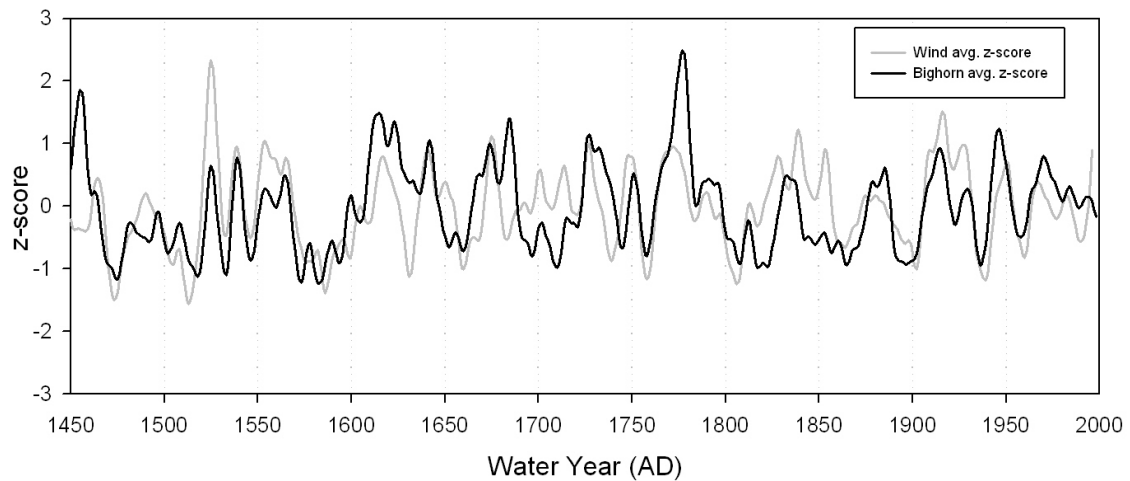
Figure 5. Z-score plots of streamflow reconstructions, grouped by mountain range and smoothed with 10-year spline algorithm.

## Relationship to Oceanic Climate Variability

Several studies suggest that climate variability in the western US can be linked to low- and high-frequency changes in sea-surface temperature and pressure anomalies in the tropical and North Pacific Ocean, with modifying influences from Atlantic Basin sea surface temperatures (Cayan et al., 1998; Graumlich et al., 2003; Gray et al., 2004; McCabe et al., 2004). The hydrologic regime of the western US is influenced to some degree by four dominant modes of Northern Hemisphere sea-surface temperature variability: the El Niño Southern Oscillation (ENSO), the Pacific Decadal Oscillation (PDO), the Atlantic Multidecadal Oscillation (AMO), and the North Atlantic Oscillation (NAO) (Hunter et al., 2006). Of these patterns, the PDO index (Mantua et al., 1997) appears to describe the strongest decadal mode of Pacific sea-surface temperatures, and studies have shown a strong PDO correlation with Northern Rockies hydrology

(Graumlich et al., 2003; Gray et al., 2003; McCabe et al., 2004; Pederson et al., 2011).

Variations in northern Pacific sea-surface temperatures are accompanied by changes in

the strength and position of the Aleutian Low during the winter months. This alters the

mean location of the jet stream and consequently winter storm tracks. Much of the

western US is also influenced by the higher-frequency ENSO, a sea-surface temperature

oscillation that moderates or reinforces the longer-frequency PDO (Mantua et al., 1997),

and strong ENSO signals have been found in both warm- and cold-season Northern

Rockies hydrology (Redmond and Koch, 1991; Cayan et al., 1998; McCabe and

Dettinger, 1999; Barlow et al., 2001). Research also reveals a significant teleconnection

between western US precipitation patterns and low-frequency variations in Atlantic

Ocean sea-surface temperatures (Gray et al., 2003; Gray et al., 2004; Kitzberger et al.,

2007). Such variations have been linked to fluctuations in the intensity of Atlantic

thermohaline circulation (Schlesinger and Ramankutty, 1994). The physical mechanisms

connecting Atlantic sea-surface temperatures with the Pacific are currently under study,

but it is apparent that variability in the hydrology of the interior western US cannot be

explained by Pacific sea-surface temperature indices alone.

In reconstructing Bighorn Basin precipitation, Gray et al. (2004) describe a

complex relationship between Basin hydrology and Pacific Ocean climate variability.

Low-elevation precipitation records reconstructed by tree-rings showed generally weak

correlations with both ENSO and PDO indices. More importantly, extended dry and wet

periods coincided with various combinations of the warm and cool phases of both

oscillations. To explore the relationship between streamflow and Pacific climate

variability, I correlated my reconstruction data with monthly and seasonal averages of the

SOI (Southern Oscillation Index) and the PDO index for the period 1900-2000 (Appendix

I). Since streamflows within the Wind River Range and the Bighorn Range are highly

correlated with other gages from the same range, I averaged streamflow values by range

and converted the result to z-scores. The April SOI and December-February PDO had

the highest correlations with streamflow and are plotted in Figure 6. The correlation

between Bighorn Range streamflow and the December-February PDO index is -0.24 (p =

0.02), and the correlation between Wind River Range streamflow and the PDO is -0.23 (p

= 0.02). The correlation between the April SOI and Bighorn and Wind River

streamflows is -0.17 (p = 0). The weak correlations between streamflow and both the

ENSO and PDO indices presented here agree generally with previous research (i.e., Gray

et al., 2004) suggesting that droughts (and wet periods) in the Bighorn Basin have

occurred during both warm and cool phases of Pacific Ocean sea-surface temperature

oscillations. For example, Figure 6 shows that in both 1970 (PDO cool) and 1979 (PDO

warm), streamflows were above average in the Basin. On a decadal scale, a shift from

generally cool to generally warm PDO conditions in the 1940s coincides with a short-

lived increase in Basin streamflow. A brief shift to cool PDO conditions in the late 1920s

coincides with an increase in streamflow as well. The well-documented change from

cool to warm PDO conditions in the 1970s (e.g., Pederson et al., 2011) does not coincide

with an appreciable change in Basin streamflow trends. Rather, streamflow values show

a persistent pattern of small year-to-year variations around the mean that begins in the

1960s and lasts until at least 2000. With regard to SOI, increased streamflows coincide

with strongly positive SOI values (La Niña) during some years (e.g., 1948 and 1983), and decreased streamflows are evident for some years of negative SOI values (e.g., 1922 and 1985). However, much more common are years in which the SOI index and streamflow are in opposition, such as in 1908, 1942, and 1992.
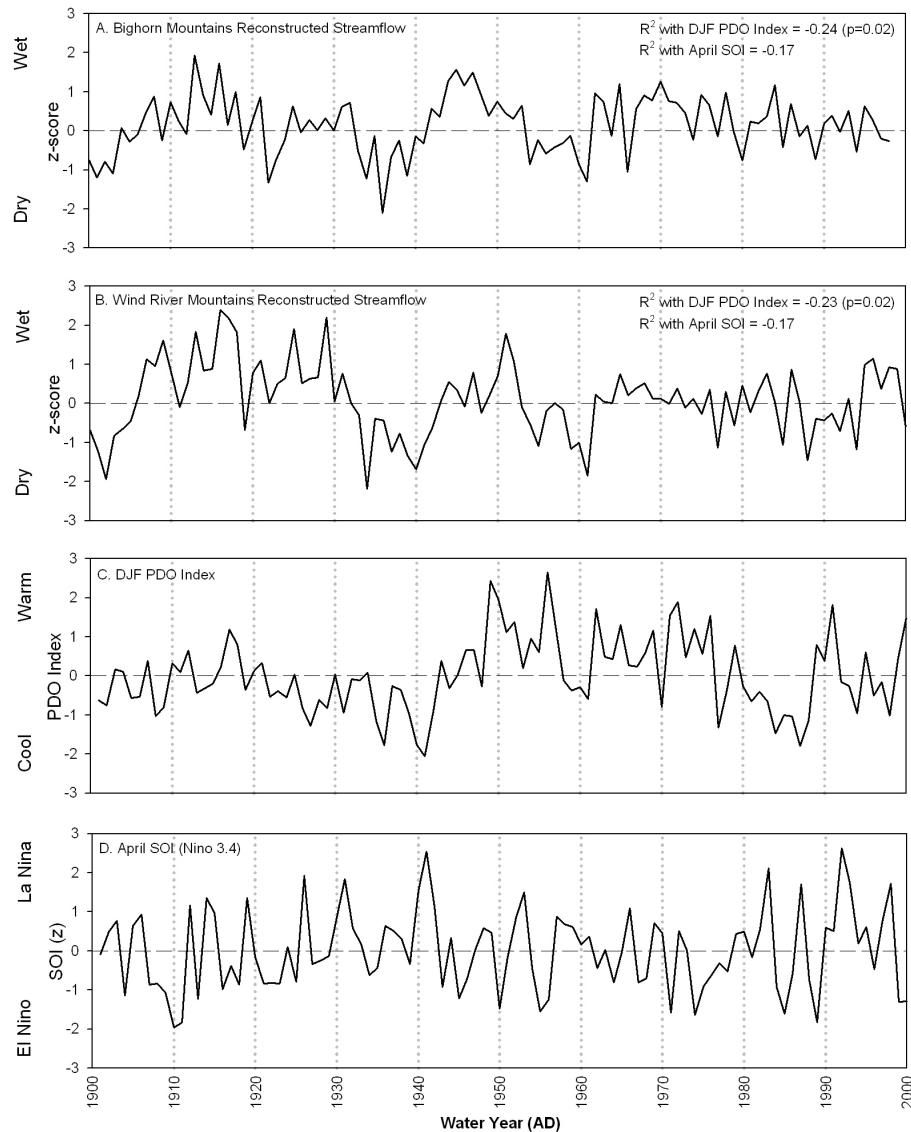


Figure 6. Comparison between streamflow reconstructions grouped by mountain range (A: Bighorn Range; B: Wind River Range), the December-February PDO index (C), and April Nino-3.4 SOI (D).

Evaluation of Wind-Bighorn Basin Water Plan Methodology

As discussed previously, the Water Plan is the current guide for water decision-making in the Bighorn Basin.  I evaluated the assumption that the 20th and 80th percentiles of the 1973-2008 gage record are representative of long-term Basin conditions by calculating the percentile values for this 36-year period for my six streamflow gage records.  I then compared the 36-year gage percentiles with the same statistics for the respective long-term reconstructions.

Table 8. Selected water-year flow statistics for the 1973-2008 gage record and the reconstructed record of each gage, in $Mm^3$.

| | **1973-2008 Gage Record** | | | | | | | |
| Gage Name | Number of Years | Std Dev | Min | 20th pctile | Mean | 80th pctile | Max | CV |
|---|---|---|---|---|---|---|---|---|
| Wind River near Dubois, WY | 28 | 42.3 | 49.5 | 96.9 | 135 | 176 | 214.9 | 31.3 |
| Bull Lake Creek above Bull Lake, WY | 36 | 59.5 | 155.8 | 183.2 | 245 | 301.1 | 370.6 | 24.3 |
| Little Bighorn River at Wyola, MT | 36 | 36.6 | 68 | 93.2 | 129 | 159.5 | 225.6 | 28.4 |
| Tongue River near Dayton, WY | 36 | 42.2 | 63.8 | 107.9 | 146.5 | 176.5 | 238.7 | 28.8 |
| Shell Creek above Shell Res., WY | 36 | 6.1 | 16 | 24 | 28.3 | 32 | 42.8 | 21.6 |
| Tensleep Creek near Tensleep, WY | 20 | 16.3 | 86.3 | 101.1 | 114.7 | 124.6 | 155.7 | 14.2 |

| | **Reconstructions** | | | | | | | |
| | Number of Years | Std Dev | Min | 20th pctile | Mean | 80th pctile | Max | CV |
|---|---|---|---|---|---|---|---|---|
| Wind River near Dubois, WY | 493 | 38.5 | 54.9 | 126.9 | 157.7 | 186.9 | 318.1 | 24.4 |
| Bull Lake Creek above Bull Lake, WY | 554 | 55.3 | 94.7 | 214.4 | 257.7 | 303.2 | 466.9 | 21.5 |
| Little Bighorn River at Wyola, MT | 829 | 33.5 | 34.8 | 88.7 | 118.5 | 145 | 240.4 | 28.3 |
| Tongue River near Dayton, WY | 829 | 38.6 | 37.4 | 111.7 | 143 | 173.6 | 297.6 | 27 |
| Shell Creek above Shell Res., WY | 749 | 7.4 | 11.6 | 25.1 | 31.5 | 37.4 | 58.6 | 23.5 |
| Tensleep Creek near Tensleep, WY | 749 | 20.4 | 64 | 95.7 | 112.8 | 129.5 | 191.2 | 18.1 |

For the Little Bighorn and Tensleep Creek gages, the long-term 20th percentiles were lower than those of the abbreviated gage record by small amounts. The 20th percentile value for the Little Bighorn reconstruction was 4.5 Mm$^3$ less than the 1973-2008 percentile value, and the Tensleep Creek 20th percentile was 5.4 Mm$^3$ less. For the remaining four gages, the 20th percentile values of the 1973-2008 gage record sufficiently bracketed those of the respective reconstructions. With regard to the 80th percentile values, the reconstructions for the Wind River, Bull Lake Creek, Shell Creek, and Tensleep Creek all revealed values higher than those of the abbreviated gage record. The largest relative difference of all the 80th percentile comparisons was for Shell Creek (5.4 Mm$^3$; 14.6% difference), and the smallest relative difference was 2.1 Mm$^3$ (0.7%) for Bull Lake Creek.

To evaluate the frequency of very dry (<20th percentile) and very wet (>80th percentile) years over the reconstructed period, each water-year was classified as such using reconstruction-derived percentile values (Table 9). The summary indicates that the 20th century was characterized by relatively few very dry years compared to previous centuries. In the case of the Little Bighorn, only six years in the 20th century were considered very dry, while 22 years were considered very wet. The other gages showed at least just as many very wet as very dry years, with the Tongue and Wind Rivers showing 22 wet years each. This view of the data suggests that, while the 1973-2008 gage record of the Bighorn Basin may provide a reasonable reference period for calculating total water-year flow averages and percentiles, the 20th century as a whole contains relatively few dry years compared with previous centuries.

Table 9. Number of very dry (20th percentile or less) and very wet (80th percentile or above) years in each reconstruction, by century.

| Century (AD) | Tongue River Dry | Wet | Little Bighorn River Dry | Wet | Shell Creek Dry | Wet | Tensleep Creek Dry | Wet | Bull Lake Creek Dry | Wet | Wind River Dry | Wet |
|---|---|---|---|---|---|---|---|---|---|---|---|---|
| 1100-1199 | 2[a] | 2 | 3[a] | 3 | | | | | | | | |
| 1200-1299 | 33 | 19 | 24 | 25 | 11[b] | 12 | 13[b] | 11 | | | | |
| 1300-1399 | 15 | 25 | 13 | 30 | 13 | 20 | 14 | 21 | | | | |
| 1400-1499 | 20 | 25 | 23 | 16 | 25 | 17 | 25 | 18 | 10[c] | 4 | | |
| 1500-1599 | 31 | 10 | 32 | 10 | 33 | 9 | 37 | 6 | 30 | 19 | 26[d] | 22 |
| 1600-1699 | 10 | 35 | 16 | 33 | 13 | 28 | 9 | 29 | 16 | 25 | 22 | 17 |
| 1700-1799 | 12 | 24 | 18 | 22 | 13 | 31 | 13 | 34 | 14 | 28 | 16 | 25 |
| 1800-1899 | 35 | 4 | 31 | 5 | 24 | 15 | 26 | 9 | 24 | 14 | 16 | 12 |
| 1900-1999 | 7 | 22 | 6 | 21 | 17 | 17 | 12 | 21 | 16 | 21 | 18 | 22 |

[a] Reconstruction begins at AD 1168

[b] Reconstruction begins at AD 1250

[c] Reconstruction begins at AD 1447

[d] Reconstruction begins at AD 1507

## 5. DISCUSSION

Results from this study show that growth data from long-lived trees in the Rocky Mountain region are highly correlated with the gage record of Bighorn Basin streamflow and can be used as a reasonable proxy for Basin hydrology over the last 800 years. Extending the record of streamflow back in time beyond the gage period offers new information on the natural temporal and spatial variability of hydrologic conditions in the Basin. Such information has implications for the way water is managed in the Bighorn Basin. In this section, I will discuss the nature of drought in the context of both the long-term and the instrumental record. I will also discuss differences in streamflow from the mountain ranges surrounding the Basin, as well as the relationship between Basin hydrology and oceanic climate indices. Implications for Basin water management are also reviewed, as are the various ways in which data from the streamflow reconstructions can be applied to water planning. Finally, I discuss the potential effects of climate warming on the hydrologic system.

### Drought in the Bighorn Basin

The character of both single- and multi-year dry and wet events apparent in Bighorn Basin streamflow reconstructions of the last 800 years indicates that the 20th century instrumental record is not entirely representative of long-term hydrologic variability. This finding is supported by previous tree-ring-based streamflow reconstruction studies of the Greater Yellowstone region (Graumlich et al., 2003; Gray et al., 2004; Gray et al., 2007; Watson et al., 2009), which show that the 20th century has

been relatively wet compared to previous centuries.  My study adds new evidence for the occurrence of droughts with greater severity than any event captured by the instrumental record, including the 2000s, 1930s and 1950s droughts.  Indeed, drought events lasting longer than a decade appear to have been common before the 20th century.  According to the event scores (Table 6), pre-instrumental droughts consistently exceeded 20th century events in terms of their exceptional duration, total deficit, and intensity values.  For example, the winter of 1999-2000 began a multi-year run of below-average streamflow in much of the Northern Rockies, including the Bighorn Basin.  During this event, the springtime peak volume of both Bighorn Lake and Boysen Reservoir (the largest reservoirs in the Basin) decreased steadily and did not recover to pre-drought levels until 2009 (Bureau of Reclamation, 2011).  Although this basin-wide event was the worst recorded in the 20th century, my reconstructions suggest that droughts of equal duration, severity and spatial extent were common on longer timescales.  According to the event scores calculated for the gage record and tree-ring-based record, the early-2000s drought had a score ranging from 73 to 121, depending on the gage.  For comparison, the 16th century "megadrought" had a score ranging from 76 to 128, and the 13th century drought event scored as high as 137 in the case of the Little Bighorn.  Thus, the reconstructions indicate that the event in the early 2000s was not unprecedented.  The streamflow reconstructions also show sudden shifts between extreme wet and dry periods, on both yearly and decadal timescales.  For example, the combined decrease in streamflow from 1617 to 1618 evident in the Bighorn Range reconstructions exceeded 360 Mm$^3$.  Shifts of

such magnitude have not occurred in the 20th century. Further, both the 1930s and 1950s droughts were preceded by extended periods of above-average flow years.

Adding to the high variability in total water supply is the potential for significant differences in the contribution of streamflow from the Wind River and Bighorn ranges during the same year. Although relatively rare, the reconstructions show years (e.g., AD 1529, 1669, 1747, 1841) in which very high (>80th percentile) runoff from one range was paired with low (<20th percentile) runoff from the other. These occasional strong spatial differences in runoff between the Wind River and Bighorn ranges may be attributed to interannual variability in the synoptic climate patterns that drive hydrologic variability across the Rocky Mountains as a whole. During some years, the southerly low-level jet from the central US may deliver abundant moisture to the Bighorn Range but less to the Wind River Range. As a result, the ranges may accumulate significantly different amounts of precipitation in the spring-early summer season. However, as mentioned previously, neither the gage record nor the reconstructions reveals periods lasting more than a year or two at a time in which streamflow differs significantly between the ranges.

Poor correlations between Bighorn Basin streamflow and oceanic climate indices add more evidence that the relationship between Basin hydrology and Pacific Ocean climate variability is complex. Although the strong effect of the PDO on winter precipitation in the Northern and Central Rocky Mountains is well-documented (i.e., years with high snowpack tend to be associated with the cool phase of the PDO), superimposed on the PDO/streamflow relationship is the effect of higher-frequency variations in the ENSO. In the Bighorn Basin, winter precipitation in the mountains

shows a moderate correlation with ENSO (Gray et al., 2004), with higher snowpack and runoff often occurring during the cool phase (La Niña). My work finds a similar relationship with streamflow, but the correlations are much weaker. Furthermore, previous work by Woodhouse (2001) and Gray et al. (2004) suggests that, on interannual time scales, lowland precipitation in the Central Rocky Mountains responds to ENSO forcing in much the same way that is seen in the southwestern US (wet during ENSO warm phase), while high-elevation areas typically show the opposite response (wet during ENSO cool phase, i.e., La Niña). These patterns suggest that streamflow, driven largely by mountain snowpack, should be highest when both the PDO and ENSO are in cool phase. However, possibly because the Bighorn Basin is located within the Central Rocky Mountain region and also near the southwestern US region, the statistical relationships between streamflow, PDO, and ENSO are not clear. Additionally, the effect of Pacific Ocean climate variability on Basin streamflow is likely moderated or enhanced by poorly-understood teleconnections with the Atlantic (Gray et al., 2004), as well as interannual variability in the low-level jet. Such complexity limits the potential for long-range hydrologic forecasting in the Bighorn Basin at the present time.

<p style="text-align:center;">Implications for Bighorn Basin Water Management</p>

The prevalence of significant interannual and decadal variability throughout the last 800 years should interest water managers in the Bighorn Basin as they plan for the future. Severe single-year droughts in the past likely placed extreme stress on aquatic and terrestrial ecosystems. However, with a well-developed system of reservoirs in

place, the Basin is capable of withstanding dry periods between one and several years in duration.  Indeed, many of the reservoirs were built as a response to the 1950s drought. However, as evidenced by the early-2000s drought, the Basin is very susceptible to multi-year runs of sustained low streamflow, especially if flow is significantly below average in any given drought year.  Given the considerable stress placed on Basin water supplies by the early-2000s drought, an event equaling or exceeding the severe pre-instrumental droughts revealed by tree-ring reconstructions would likely lead to unprecedented water shortages, even with the storage offered by the current network of reservoirs.  The effects in the state of Wyoming would likely be exacerbated by the requirements of the Yellowstone River Compact of 1950, under which Wyoming is obligated to allow a substantial quantity of Bighorn River flow to pass through to Montana and North Dakota, even in severe drought years.

Although relatively rare, the reconstructions reveal brief periods in which streamflow from the Wind River Range and the Bighorn Range is significantly different. If strong spatial heterogeneity in streamflow were to occur in the future and last for several years, it would present water managers with a challenging situation.  For example, if Bighorn Range streamflows were severely low and Wind River Range streamflows abnormally high, the lower Bighorn Basin (downstream of Boysen Reservoir) would need more supply from the upper Basin (the Wind River drainage) than normal.  However, senior water rights holders in the upper Basin, especially the Wind River Indian Reservation, may not be legally obligated to release the needed water. Conversely, if Wind River Range runoff was abnormally low while Bighorn Range

runoff was high, the lower Basin would need to reduce water consumption such that the upper Basin could withhold more to satisfy its own needs.  This would essentially 'transfer' water from the lower to the upper Basin via operational means, rather than physical means.

With regard to the Wind-Bighorn Basin Water Plan, my findings support the ability of current planning thresholds to sufficiently capture the long-term variability in single-year streamflow, even considering the longer timescale offered by tree-ring analysis.  Use of the 1973-2008 gage record of the Basin to characterize dry, average, and wet hydroclimatic conditions for planning purposes is supported by my analysis.  The adequacy of the 1973-2008 reference period is a result of the wide range of both wet and dry flow values that occurred during this timeframe.  Indeed, years of both extremely high (e.g., 1986) and low (e.g., 2001) flow occurred during this period.  However, multiple analyses presented here suggest that a more-sophisticated method of defining worst-case water-supply scenarios would improve water-system resiliency under drought conditions.  Drought-quantification techniques, such as event scoring, consider not only the range of flows possible for any given year (as the Water Plan does), but also account for the cumulative impacts of events spread out over longer timescales. Event scores from tree-ring-based streamflow reconstructions indicate that droughts can occur in various combinations of event duration, cumulative deficit, and intensity.  Therefore, viewing hydroclimatic variability in terms of events rather than years offers a more-robust approach to identifying water-supply vulnerabilities.  In the next section I discuss ways in which these reconstructions can be used to directly inform the Water Plan.

Potential Applications for Streamflow Reconstructions

As the amount of paleohydrologic research grows, so does interest in using such

information to directly inform natural resource management.  Tree-ring-based streamflow

reconstructions are increasingly used to better manage water resources in many areas of

the western US, especially the Colorado River basin (Woodhouse and Lukas, 2006).

Here, collaborative relationships between paleoclimatologists and water resource

managers are improving the accessibility, understanding, and utilization of paleoclimatic

data in water management, while also providing feedback to researchers about how their

work can be more practically useful.  Tree-ring-based streamflow reconstructions can be

made relevant in two ways: quantitatively, such as through inclusion of paleohydrologic

data in water models, and qualitatively by including reconstructions as part of educational

outreach to water-management boards and the public in general (Table 10).

Table 10. Applications for tree-ring-based streamflow reconstructions.  Adapted from the
NOAA TreeFlow project (Woodhouse and Lukas, 2011).

| Type of Application | Example Activity | Audience | Potential Outcome |
|---|---|---|---|
| Qualitative Guidance | Plots, graphs, and maps of tree-ring-based hydrologic reconstructions for education and communication | Irrigators, local government officials, water-policy decisionmakers | Better appreciation for natural hydrologic variability; better policymaking |
| Quantitative Assessment | Standardizing drought events across the gaged and reconstructed record using an event scoring technique, then comparing the 20th century with the past | General audience | Better appreciation for natural hydrologic variability, improved context for the 20th century gage record; better policymaking |
| Model Input | Evaluate numerical water-management models using reconstructed hydrology to 'test' them under severe drought conditions | Water system engineers, including dam operators | More resilient water supply systems under challenging climate scenarios; higher system efficiency |

In a survey of water-management groups in Colorado, New Mexico, Arizona, and Wyoming, Rice et al. (2009) found that paleohydrologic information improved understanding of the substantial hydrologic variability possible in the western US. Additionally, water managers are re-examining the long-held assumption that the 1950s drought was the 'worst-case scenario.'

As with many scientific disciplines, however, significant barriers complicate the translation of science to water policy. The successful inclusion of paleoclimatic data in water-resource decision-making relies on the ability of scientists to communicate their findings with planners at appropriate temporal and spatial scales and on the capacity, knowledge, and willingness of stakeholders (Gamble et al., 2003). For example, in some basins the hesitation to adopt proxy-based reconstructions into policymaking is based on the notion that tree-ring science involves too much uncertainty or is otherwise not credible, a belief that is often driven by localized cultural norms (Rice et al., 2009). As evidenced in the southwestern US (particularly Colorado), such challenges can often be overcome by a 'coproduction' approach for science and policy, where the paleoclimatic research agenda is developed collaboratively between scientists and decision-makers. Such a process reflects the understanding that the useful integration of paleoclimatic information into water resource planning is much more likely if an interactive research environment exists, rather than the traditional one-way dissemination process (Rice et al., 2009).

Water-management agencies have used a number of approaches to incorporate information from tree-ring reconstructions into water-management plans. Rice et al.

(2009) found that the majority of all groups that were made aware of paleohydrologic reconstructions were at least qualitatively using the information to educate stakeholders about longer-term drought characteristic of western watersheds. It has also helped convey the range of uncertainty inherent in western US hydrology to the public, as well as place reasonable bounds on expectations for the future. Quantitatively, several water utilities have used paleohydrologic data as inputs into their operational water distribution models as a way to test their reliability under drought conditions. For example, rather than calculate water system stress using the minimum streamflows of the 1950s, managers of a particular water district (anonymous; see Rice et al., 2009) in Colorado used the estimated flow volumes of the 1840s drought instead. Water rationing would not be necessary based on the 1950s worst-case scenario, but the 1840s event challenged that assumption and spurred changes in the utility's drought plan. Also, novel ways of combining historic with paleoreconstructed streamflow data have been developed for use in stochastic streamflow models (Prairie et al., 2008). Such efforts attempt to overcome the real and perceived reliability issues associated with traditional regression-based reconstruction methods.

Similar qualitative and quantitative approaches to using tree-ring reconstructions of streamflow could be employed in the Bighorn Basin. With some modifications, the new 'worst-case' streamflow scenarios presented by these reconstructions could be used as direct inputs into the models used to develop the Water Plan. Although this study reconstructed only a subset of the streamflow gages used to develop the Water Plan, the results from each can be disaggregated and scaled to match those used in existing flow

models. In other words, reconstruction-based estimates of low and high streamflow could be used in place of gage-based data for the five reconstructed sub-basins that fall within the Wind-Bighorn Basin boundary. For the rest of the sub-basins, it may be possible to translate the reconstructions using a scaling approach, much in the same way that rainfall-runoff models are created.

## Future Hydrology Under a Warming Climate

An important consideration for water managers is how Bighorn Basin water supplies might be affected under the temperature increases projected in the coming decades. Down-scaled climate model projections suggest that the major river basins of the western US will experience average annual temperatures 2° C higher than present by 2050 (Barnett et al., 2004). The most significant negative impact of warming will likely be a reduction in mountain snowpack (specifically, snow water equivalent (SWE)) and an attendant reduction in natural storage. This warming trend has been underway since the 1950s (Mote et al., 2005; Pierce et al., 2008) and is associated with a shift towards earlier timing of peak snowmelt, as well as an increase in the number of frost-free ($\geq 0°C$) and snowcover-free days in the Rocky Mountains (Pederson et al., 2011). Accompanying these trends are indications that an increasing percentage of total water-year discharge now occurs in winter (Stewart et al., 2005), due in part to an increase in the proportion of annual precipitation falling as rain rather than snow (Knowles et al., 2006). Based on this regional information, average spring hydrographs for streamflow gages in the Bighorn Basin are likely to elongate (since more streamflow will occur in the winter) and flatten

(due to the diminished effect of the typical springtime snowmelt pulse). The earlier loss of yearly snowpack will also contribute to negative glacier mass balance, and the loss of natural water storage in the Wind River glacier complex will continue to diminish. Wind River glaciers have been retreating since the 1930s (Marston et al., 1989). Given the substantial contribution of glacier meltwater to Bighorn Basin runoff, the Basin may be disproportionately affected by the current warming trend if the glaciers disappear completely. Water managers will need to adjust the water storage and distribution system of the entire Basin if the timing and quantity of Wind River runoff changes due to loss of glaciers. The extended records of hydroclimatic information presented by this study suggest that current water-management plans could be modified to better reflect the true nature of hydrologic variability in the Basin, thereby increasing the resiliency of Basin water supplies under a warmer future.

## 6. CONCLUSIONS

This research presents the first tree-ring-based streamflow reconstructions for the Bighorn Range and updates two previous reconstructions from the Wind River Range. Together, the reconstructions provide a comprehensive paleohydrologic record for the Bighorn Basin as a whole.  The reconstructions reveal substantial hydrologic variability in terms of both event duration and event magnitude since the early 13$^{th}$ century, a finding that is consistent with several other tree-ring-based streamflow reconstructions from the Northern Rockies.

In terms of individual years, these reconstructions suggest that the driest years of the 20$^{th}$ (and 21$^{st}$) centuries were similar in severity to the driest years of the last eight centuries.  However, preinstrumental multi-year and decadal-scale droughts were commonly longer in duration and/or more severe in magnitude than any in the gage record.  Additionally, these droughts represent water deficits that have no analog in the modern record, even considering the uncertainties associated with tree-ring-based flow estimates.  Furthermore, while there is evidence that single-year droughts may have been restricted to a particular region of the Bighorn Basin, multi-year and decadal drought events affected the entire watershed.  The reconstructions also indicate that rapid switching from extended wet to extended dry streamflow regimes was a common feature of past hydrology in the Basin, and dramatic changes in streamflow occurred in as little as one year (e.g., from 1617 high flow to 1618 low flow).  The pre-instrumental streamflow statistics also highlight the general wetness of the modern record compared with the previous 800 years.

This study also suggests that current water planning guidance in use by the Wind-Bighorn Basin would benefit from the expanded perspective offered by these streamflow reconstructions. According to my analysis, the 1973-2008 gage record of the Basin serves as a fairly representative period with which to calculate water supplies under different climate scenarios. Indeed, this 36-year record includes a wide range of annual streamflow values in the gages I reviewed. Therefore, the percentile thresholds for the gage record compare favorably with those for the reconstructed record. However, the Water Plan does not account for the types of multi-year drought events seen so frequently throughout the reconstructed record. Information from the event score tables presented here can improve the ability of the Basin water-supply system to anticipate not only single dry years, but also severe multi-year water deficits. Furthermore, the streamflow estimates presented by these reconstructions can be disaggregated and used as inputs for the Water Plan, improving the ability of water managers to identify system vulnerabilities.

Overall, this work illustrates the value of incorporating long-term paleoclimatic information into water-resources management. Tree-ring-based reconstructions offer a robust means of developing more realistic scenarios for droughts and wet periods, and can therefore be used to identify weaknesses in current water management systems. Despite uncertainties in climate projections at the regional scale (Kerr, 2011), the ability to view hydrologic variability in a temporal context broader than that offered by the gage record gives water managers, users, and policy makers an opportunity to develop

sustainable water-management practices that satisfy the needs of both the economy and
the environment.

REFERENCES CITED

Alley, W. 1984. The Palmer Drought Severity Index: Limitations and Assumptions. Journal of Climate and Applied Meteorology 23: 1100-1109.

Barlow, M., S. Nigam, and E. Berberry. 2001. ENSO, Pacific Decadal Variability, and U.S. Summertime Precipitation, Drought, and Stream Flow. Journal of Climate 14 (9): 2105-2129.

Barnett, F., S. Gray, and G. Tootle. 2010. Upper Green River Basin (United States) Streamflow Reconstructions. Journal of Hydrologic Engineering 15 (7): 567-579.

Barnett, T., R. Malone, W. Pennell, D. Stammer, B. Semtner, and W. Washington. 2004. The Effects of Climate Change on Water Resources in the West: Introduction and Overview. Climatic Change 62 (1): 1–11.

Biondi, F., T. Kozubowski, and A. Panorska. 2002. Stochastic Modeling of Regime Shifts. Climate Research 23: 23-30.

Bonin, D., and D. Burn. 2005. Use of Tree Ring Reconstructed Streamflows to Assess Drought. Canadian Journal of Engineering 32 (6): 1114-1123.

Box, G., and G. Tiao. 1975. Intervention Analysis with Applications to Economic and Environmental Problems. Journal of the American Statistical Association 70 (349): 70-79.

Bradley, R. 1999. Paleoclimatology: Reconstructing Climates of the Quaternary. Second Ed. Vol. 68. Academic Press.

Bureau of Land Management. 2001. Wyoming Water Rights Fact Sheet. Wyoming Water Rights Fact Sheet. http://www.blm.gov/nstc/WaterLaws/wyoming.html.

Bureau of Reclamation. 2011. HYDROMET Data System. Washington, D.C., U.S.A.: Bureau of Reclamation. http://www.usbr.gov/gp/hydromet/.

Carson, E., and J. Munroe. 2005. Tree-ring Based Streamflow Reconstruction for Ashley Creek, Northeastern Utah: Implications for Palaeohydrology of the Southern Uinta Mountains. The Holocene 15 (4): 602.

Case, R., and G. MacDonald. 2003. Tree Ring Reconstructions Of Streamflow for Three Canadian Prairie Rivers. Journal of the American Water Resources Association 39 (3): 703–716.

Cayan, D., M. Dettinger, H. Diaz, and N. Graham. 1998. Decadal Variability of Precipitation Over Western North America. Journal of Climate 11: 3148–3166.

Cook, E. 2004. Long-Term Aridity Changes in the Western United States. Science 306: 1015-1018. doi:10.1126/science.1102586.

Cook, E., and G. Jacoby. 1983. Potomac River Streamflow Since 1730 as Reconstructed by Tree Rings. Journal of Climate and Applied Meteorology.

Cook, E., and L. Kairiukstis. 1990. Methods of Dendrochronology: Applications in the Environmental Sciences. Netherlands: Springer.

Cook, E., D. Meko, D. Stahle, and M. Cleaveland. 1999. Drought Reconstructions for the Continental United States. Journal of Climate 12: 1145–1162.

Dracup, J., K. Lee, and E. Paulson, Jr. 1980. On the Statistical Characteristics of Drought Events. Water Resources Research 16 (2): 289-296.

Draper, N., and H. Smith. 1998. Applied Regression Analysis. 3rd ed. New York: John Wiley.

DRI. 2009. Westmap. WestMap Climate Analysis and Mapping Toolbox. http://cefa.dri.edu/Westmap/.

Easterling, D., and T. Peterson. 1995. A New Method of Detecting Undocumented Discontinuities in Climatological Time Series. International Journal of Climatology 15: 369-377.

Fritts, H. 1976. Tree Rings and Climate. London: Academic Press.

Gamble, J., J. Furlow, A. Snover, A. Hamlet, B. Morehouse, H. Hartmann, and T. Pagano. 2003. Assessing the Impact of Climate Variability and Change on Regional Water Resources: The Implications for Stakeholders. In Water: Science, Policy, and Management, 341-658. Washington, D.C.: American Geophysical Union.

Gedalof, Z., D. Peterson, and N. Mantua. 2004. Columbia River Flow and Drought Since 1750. Journal of the American Water Resources Association 40 (6): 1579-1592.

Graumlich, L., M. Pisaric, L. Waggoner, J. Littell, and J. King. 2003. Upper Yellowstone River Flow and Teleconnections with Pacific Basin Climate Variability During the Past Three Centuries. Climatic Change 59 (1): 245–262.

Gray, S., J. Betancourt, C. Fastie, and S. Jackson. 2003. Patterns and Sources of Multidecadal Oscillations in Drought-sensitive Tree-ring Records from the Central and Southern Rocky Mountains. Geophysical Research Letters 30 (6): 1316.

Gray, S., C. Fastie, S. Jackson, and J. Betancourt. 2004. Tree-ring-based Reconstruction of Precipitation in the Bighorn Basin, Wyoming, Since 1260 AD. Journal of Climate 17: 3855–3865.

Gray, S., L. Graumlich, and J. Betancourt. 2007. Annual Precipitation in the Yellowstone National Park Region Since AD 1173. Quaternary Research 68 (1): 18–27.

Gray, S., L. Graumlich, J. Betancourt, and G. Pederson. 2004. A Tree-ring Based Reconstruction of the Atlantic Multidecadal Oscillation Since 1567 AD. Geophysical Research Letters 31 (12): L12205.

Gray, S., S. Jackson, and J. Betancourt. 2004. Tree-ring Based Reconstructions of Interannual to Decadal Scale Precipitation Variability for Northeastern Utah Since 1226 AD. Journal of the American Water Resources Association 40 (4): 947–960.

Gray, S. 2010. Personal Communication.

Guttman, N., and R. Quayle. 1996. A Historical Perspective of U.S. Climate Divisions. Bulletin of the American Meteorological Society 77: 293-303.

Haan, C. 2001. Statistical Methods in Hydrology. 2nd ed. Ames, Iowa: Iowa State University Press.

Hirsch, R. 1979. An Evaluation of Some Record Reconstruction Techniques. Water Resources Research 15 (6): 1781-1790.

Hirsch, R., and J. Costa. 2004. U.S. Stream Flow Measurement and Data Dissemination Improve. EOS: Transactions of the American Geophysical Union 85 (21): 197-203.

Hunter, T., G. Tootle, and T. Piechota. 2006. Oceanic-atmospheric Variability and Western U.S. Snowfall. Geophysical Research Letters 33: L13706.

Jacobs, J., and D. Brosz. 1993. Wyoming's Water Resources. Cooperative Extension Service, College of Agriculture and Wyoming Water Resources Center, University of Wyoming.

Jain, S., C. Woodhouse, and M. P Hoerling. 2002. Multidecadal Streamflow Regimes in the Interior Western United States- Implications for the Vulnerability of Water Resources. Geophysical Research Letters 29 (21): 32–1.

Kerr, R. 2011. Vital Details of Global Warming Are Eluding Forecasters. Science 334 (6053) (October 14): 173-174.

Kitzberger, T., P. Brown, E. Heyerdahl, T. Swetnam, and T. Veblen. 2007. Contingent Pacific–Atlantic Ocean influence on Multicentury Wildfire Synchrony over Western North America. Proceedings of the National Academy of Sciences 104 (2): 543.

Knight, T., G. Policy, and P. Center. 2004. Reconstruction of Flint River Streamflow Using Tree-rings. Water Policy Working Paper, Georgia Water Policy and Planning Center.

Knowles, N., M. Dettinger, and D. Cayan. 2006. Trends in Snowfall versus Rainfall in the Western United States. Journal of Climate 19: 4545-4559.

Lawrence, C. 1987. Streamflow Characteristics at Hydrologic Benchmark Stations. US Geological Survey Circular 941, 123 p.

Lins, H. 1997. Regional Streamflow Regimes and Hydroclimatology of the United States. Water Resources Research 33 (7): 1655-1667.

Loáiciga, H. 1993. Dendrohydrology and Long-Term Hydrologic Phenomena. Reviews of Geophysics 31 (2): 151-171.

Loáiciga, H. 2005. Drought, Tree Rings, and Reservoir Design. Journal of the American Water Resources Association 41 (4): 949–958.

Maffly, B. 2007. Battle on the Bighorn. Montana Outdoors. http://fwp.mt.gov/mtoutdoors/HTML/articles/2007/bighornriver.htm.

Maidment, D. 1993. Handbook of Hydrology. New York: McGraw-Hill.

Mantua, N., S. Hare, Y. Zhang, J. Wallace, and R. Francis. 1997. A Pacific Interdecadal Climate Oscillation with Impacts on Salmon Production. Bulletin of the American Meteorological Society 78 (6): 1069-1079.

Marston, R., L. Pochop, G. Kerr, and M. Varuska. 1989. Long-Term Trends in Glacier and Snowmelt Runoff, Wind River Range, Wyoming. Project Report for the Wyoming Research Center. University of Wyoming.

McCabe, G., and M. Dettinger. 1999. Decadal Variations in the Strength of ENSO Teleconnections with Precipitation in the Western United States. International Journal of Climatology 19 (13): 1399-1410.

McCabe, G., M. Palecki, and J. Betancourt. 2004. Pacific and Atlantic Ocean Influences on Multi-Decadal Drought Frequency in the United States. Proceedings of the National Academy of Sciences 101 (12): 4136-4141.

Meko, D., C. Stockton, and W. Boggess. 1995. The Tree-Ring Record of Severe Sustained Drought. Journal of the American Water Resources Association 31 (5): 789-801.

Meko, D., M. Therrell, C. Baisan, and M. Hughes. 2001. Sacramento River Flow Reconstructed to AD 869 From Tree Rings. Journal of the American Water Resources Association 37 (4): 1029–1039.

Meko, D., C. Woodhouse, C. Baisan, T. Knight, J. Lukas, M. Hughes, and M. Salzer. 2007. Medieval Drought in the Upper Colorado River Basin. Geophysical Research Letters 34 (10): 10705.

Mock, C. 1996. Climatic Controls and Spatial Variations of Precipitation in the Western United States. Journal of Climate 9: 1111-1125.

Mote, P., A. Hamlet, M. Clark, and D. Lettenmaier. 2005. Declining Mountain Snowpack in Western North America. Bulletin of the American Meteorological Society 86 (1): 39.

National Oceanic and Atmospheric Administration. 2011. National Climatic Data Center. Asheville, NC: National Oceanic and Atmospheric Administration. http://www.ncdc.noaa.gov/oa/ncdc.html.

NCAR. 2011. El Nino: The El Nino - Southern Oscillation. http://www.cgd.ucar.edu/cas/ENSO/enso.html.

Palmer, W. 1965. Meteorological Drought. Washington, D.C.: Office of Climatology, U.S. Weather Bureau.

Pederson, G., S. Gray, T. Ault, W. Marsh, D. Fagre, A. Bunn, C. Woodhouse, and L. Graumlich. 2011. Climatic Controls on the Snowmelt Hydrology of the Northern Rocky Mountains, USA. Journal of Climate 0: 1-22.

Pierce, D., T. Barnett, H. Hidalgo, T. Das, C. Bonfils, B. Santer, and G. Bala. 2008. Attribution of Declining Western U.S. Snowpack to Human Effects. Journal of Climate 21: 6425-6444.

Prairie, J., K. Nowak, B. Rajagopalan, U. Lall, and T. Fulp. 2008. A Stochastic Nonparametric Approach for Streamflow Generation Combining Observational and Paleoreconstructed Data. Water Resources Research 44: W06423.

PRISM Group. 1990. PRISM Group. Oregon State University. http://www.prismclimate.org.

Redmond, K., and R. Koch. 1991. Surface Climate and Streamflow Variability in the Western United States and Their Relationship to Large-Scale Circulation Indices. Water Resources Research 27 (9): 2381-2399.

Rice, J., C. Woodhouse, and J. Lukas. 2009. Science and Decision Making: Water Management and Tree-Ring Data in the Western United States. Journal of the American Water Resources Association 45 (5): 1248–1259.

Schlesinger, M., and N. Ramankutty. 1994. An Oscillation in the Global Climate System of Period 65-70 Years. Nature 367: 723-727.

Schubert, S., H. Helfand, C.-Y. Wu, and W. Min. 1998. Subseasonal Variations in Warm-Season Moisture Transport and Precipitation Over the Central and Eastern United States. Journal of Climate 11 (10): 2530-2555.

Slack, J., A. Lumb, and J. Landwehr. 1993. Hydro-Climatic Data Network (HCDN) Streamflow Data Set, 1874-1998. Reston, Virginia, U.S.A.: U.S. Geological Survey. http://www.daac.ornl.gov.

Stahle, D., E. Cook, M. Cleaveland, M. Therrell, D. Meko, H. Grissino-Mayer, E. Watson, and B. Luckman. 2000. Tree-Ring Data Document 16th Century Megadrought Over North America. EOS: Transactions of the American Geophysical Union 81 (12): 121-125.

Stewart, I., D. Cayan, and M. Dettinger. 2005. Changes Toward Earlier Streamflow Timing Across Western North America. Journal of Climate 18: 1136–1155.

Stockton, C., and G. Jacoby. 1976. Long-term Surface Water Supply and Streamflow Trends in the Upper Colorado River Basin. Lake Powell Research Project Bulletin.

Timilsena, J., T. Piechota, H. Hidalgo, and G. Tootle. 2007. Five Hundred Years of Hydrological Drought in the Upper Colorado River Basin. Journal of the American Water Resources Association 43 (3): 798-812.

USEPA. 2011. Hydraulic Fracturing Background Information. http://water.epa.gov/type/groundwater/uic/class2/hydraulicfracturing/wells_hydro what.cfm.

USGS. 2009. USGS Water Data for the Nation. http://waterdata.usgs.gov/nwis.

USHCN. 2009. United States Historical Climatology Network. Long-Term Daily and Monthly Climate Records from Stations Across the Contiguous United States. http://cdiac.ornl.gov/epubs/ndp/ushcn/access.html.

Walters, C., J. Winkler, R. Shadbolt, J. van Ravensway, and G. Bierly. 2008. A Long-Term Climatology of Southerly and Northerly Low-Level Jets for the Central United States. Annals of the Association of American Geographers 98 (3): 521-552.

Watson, T., F. Anthony Barnett, S. Gray, and G. Tootle. 2009. Reconstructed Streamflows for the Headwaters of the Wind River, Wyoming, United States. Journal of the American Water Resources Association 45 (1): 224-236.

Weisberg, S. 1985. Applied Linear Regression. 2nd ed. Hoboken, NJ: John Wiley.

Whitlock, C., and P. Bartlein. 1993. Spatial Variations of Holocene Climate Change in the Yellowstone Region. Quaternary Research 39: 231-238.

Wigley, T., K. Briffa, and P. Jones. 1984. On the Average Value of Correlated Time Series, with Applications in Dendroclimatology and Hydrometeorology. Journal of Climate and Applied Meteorology 23 (2): 201-213.

Wise, E. 2010. Tree-Ring Record of Streamflow and Drought in the Upper Snake River. Water Resources Research 46: W11529.

Woodhouse, C. 2001. A Tree-Ring Reconstruction of Streamflow for the Colorado Front Range. Journal of the American Water Resources Association 37 (3): 561–569.

Woodhouse, C. 2004. A Paleo Perspective on Hydroclimatic Variability in the Western United States. Aquatic Sciences 66 (4): 346-356.

Woodhouse, C., and J. Lukas. 2006a. Drought, Tree Rings and Water Resource Management in Colorado. Canadian Water Resources Journal 31 (4): 297–310.

Woodhouse, C., and J. Lukas. 2006b. Multi-Century Tree-Ring Reconstructions of Colorado Streamflow for Water Resource Planning. Climatic Change 78 (2-4) (August): 293-315.

Woodhouse, C., S. Gray, and D. Meko. 2006. Updated Streamflow Reconstructions for the Upper Colorado River Basin. Water Resources Research 42 (W05415): 1-16.

WSGS. 2011. Wyoming State Geological Survey. Major Rivers of Wyoming. http://www.wsgs.uwyo.edu/AboutWSGS/Major_Rivers.aspx.

WWDC. 2003. Wind-Bighorn River Basin Plan Final Report. Wyoming Water Development Commission. http://waterplan.state.wy.us/plan/bighorn/2003/finalrept/finalrept.html.

WWDC. 2010. Wind-Bighorn Basin Water Plan Update. Wyoming Water Development Commission. http://waterplan.state.wy.us/plan/bighorn/2010/finalrept/finalrept.html.

APPENDICES

APPENDIX A

CHRONOLOGY-STREAMFLOW CORRELATIONS

**These data are located on a companion CD.  If a CD is not attached to the back cover of this document, please contact your local or public university library to place an interlibrary loan request to Montana State University.  Please call 406-994-3161 with any questions.
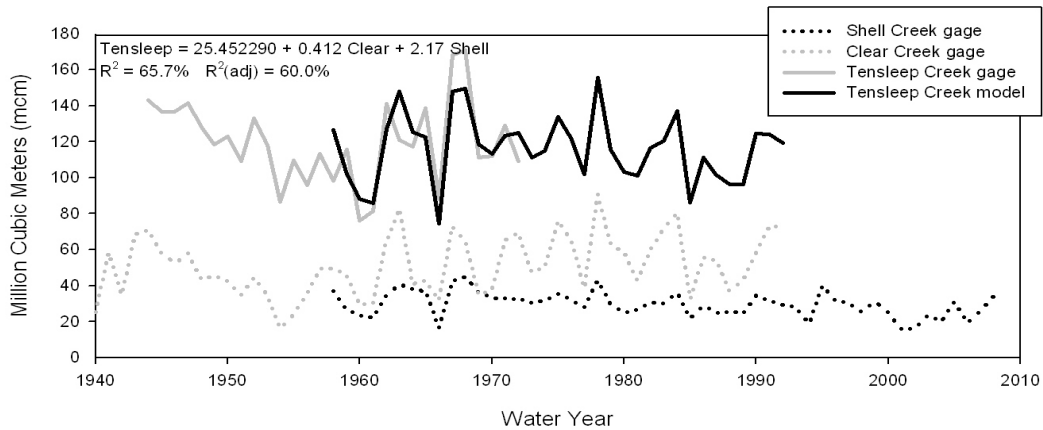
APPENDIX B


CHRONOLOGY-CLIMATE CORRELATIONS

**These data are located on a companion CD.  If a CD is not attached to the back cover of this document, please contact your local or public university library to place an interlibrary loan request to Montana State University.  Please call 406-994-3161 with any questions.

APPENDIX C


TENSLEEP CREEK DATA SYNTHESIS

Tensleep Creek flow data extension model.  The Tensleep Creek gage record ran from the 1944 water-year through the 1972 water-year and was decommissioned afterwards.  Shell Creek (USGS # 06278300) and Clear Creek (#06318500) gage records were used in a multiple-linear regression model to estimate Tensleep Creek streamflow for years 1973-1992, extending the period of record from 29 to 49 years.

The regression equation is:
TENSL = 25452290 + 0.412 CLEAR + 2.17 SHELL

15 cases used, 83 cases contain missing values

| Predictor | Coef | SE Coef | T | P | VIF |
|---|---|---|---|---|---|
| Constant | 25452290 | 20241580 | 1.26 | 0.233 | |
| CLEAR | 0.4123 | 0.3545 | 1.16 | 0.267 | 1.720 |
| SHLAB | 2.1693 | 0.7767 | 2.79 | 0.016 | 1.720 |

S = 17679431   R-Sq = 65.7%   R-Sq(adj) = 60.0%

PRESS = 6.118865E+15   R-Sq(pred) = 44.03%

<u>Analysis of Variance</u>

| Source | DF | SS | MS | F | P |
|---|---|---|---|---|---|
| Regression | 2 | 7.18091E+15 | 3.59045E+15 | 11.49 | 0.002 |
| Residual Error | 12 | 3.75075E+15 | 3.12562E+14 | | |
| Total | 14 | 1.09317E+16 | | | |

No replicates.
Cannot do pure error test.

| Source | DF | Seq SS |
|---|---|---|
| CLEAR | 1 | 4.74238E+15 |
| SHLAB | 1 | 2.43853E+15 |

Durbin-Watson statistic = 1.81212

No evidence of lack of fit (P >= 0.1).

APPENDIX D

RECONSTRUCTION MODEL EQUATIONS AND STATISTICS

See Table 1 for tree-ring chronology metadata.

WIND1:

The regression equation is
WINDB = 92648990 + 53705407 DIN  Std - 84033172 DCR  Std + 61674088 FMT  Std + 37217564 MEV
Std

47 cases used, 1593 cases contain missing values

Predictor     Coef  SE Coef    T     P   VIF
Constant    92648990  22946607   4.04  0.000
DIN  Std    53705407  16057522   3.34  0.002  1.472
DCR  Std   -84033172  28082638  -2.99  0.005  1.870
FMT  Std    61674088  21186157   2.91  0.006  1.893
MEV  Std    37217564  17023042   2.19  0.034  1.378

S = 28379388   R-Sq = 49.1%   R-Sq(adj) = 44.3%

PRESS = 4.187218E+16   R-Sq(pred) = 37.04%

Analysis of Variance

Source        DF        SS         MS       F      P
Regression     4  3.26778E+16  8.16946E+15  10.14  0.000
Residual Error  42  3.38264E+16  8.05390E+14
Total         46  6.65042E+16

Source   DF     Seq SS
DIN  Std   1  1.52626E+16
DCR  Std   1  7.47757E+14
FMT  Std   1  1.28177E+16
MEV  Std   1  3.84971E+15

---

BLAKE1:

The regression equation is
BLAKE  = 197590137 + 117899416 DIN  Std - 128980590 CFY Std + 78215883 BLE  Std

46 cases used, 1594 cases contain missing values

Predictor     Coef  SE Coef    T     P   VIF
Constant    197590137  26761477   7.38  0.000
DIN  Std    117899416  19829874   5.95  0.000  1.471
CFY  Std   -128980590  26069837  -4.95  0.000  1.460
BLE  Std    78215883  17929618   4.36  0.000  1.179

S = 33726986   R-Sq = 61.9%   R-Sq(adj) = 59.2%

PRESS = 5.769767E+16   R-Sq(pred) = 54.04%

Analysis of Variance

Source        DF        SS        MS      F      P
Regression     3  7.77646E+16  2.59215E+16  22.79  0.000
Residual Error  42  4.77754E+16  1.13751E+15
Total          45  1.25540E+17

No replicates.
Cannot do pure error test.

Source    DF      Seq SS
DIN  Std  1  3.60967E+16
CFY  Std  1  2.00206E+16
BLE  Std  1  2.16473E+16

---

## BLAKE2:

The regression equation is
BLAKE = 145656460 + 134388185 DIN  Std - 146650192 CFY Std + 122708939 MDP Std

43 cases used, 1597 cases contain missing values

Predictor      Coef  SE Coef    T      P    VIF
Constant    145656460  47225323  3.08  0.004
DIN  Std    134388185  21672375  6.20  0.000  1.323
CFY  Std    -146650192  31059175  -4.72  0.000  1.521
MDP Std     122708939  42367107  2.90  0.006  1.173

S = 36929786   R-Sq = 53.9%   R-Sq(adj) = 50.3%

PRESS = 6.242878E+16   R-Sq(pred) = 45.85%

Analysis of Variance

Source        DF        SS        MS      F      P
Regression     3  6.20993E+16  2.06998E+16  15.18  0.000
Residual Error  39  5.31886E+16  1.36381E+15
Total          42  1.15288E+17

No replicates.
Cannot do pure error test.

Source    DF      Seq SS
DIN  Std  1  2.95803E+16
CFY  Std  1  2.10784E+16
MDP Std   1  1.14406E+16

---

## LTLBG1:

The regression equation is

LTLBG = - 1984147 - 71329073 ARR Std + 69717868 CKC Std + 45984498 MEV Std + 37009544 RCU Std + 41341964 SRV Std

58 cases used, 1582 cases contain missing values

```
Predictor     Coef SE Coef    T    P   VIF
Constant   -1984147 23529723 -0.08 0.933
ARR Std   -71329073 19053135 -3.74 0.000 1.887
CKC Std   69717868 18836878  3.70 0.001 1.441
MEV Std    45984498 12283993  3.74 0.000 1.270
RCU Std   37009544 17679832  2.09 0.041 1.281
SRV Std   41341964 11844748  3.49 0.001 1.342
```

S = 23424075   R-Sq = 52.9%   R-Sq(adj) = 48.3%

PRESS = 3.510416E+16   R-Sq(pred) = 42.02%

Analysis of Variance

```
Source        DF       SS       MS       F     P
Regression     5  3.20175E+16 6.40350E+15 11.67 0.000
Residual Error 52 2.85317E+16 5.48687E+14
Total         57  6.05492E+16
```

```
Source   DF     Seq SS
ARR Std  1  1.19361E+15
CKC Std  1  1.29997E+16
MEV Std  1  9.80472E+15
RCU Std  1  1.33515E+15
SRV Std  1  6.68429E+15
```

---

## LTLBG2:

The regression equation is
LTLBG = 6476041 + 34059484 MEV Std + 40624869 CKC Std + 15206424 BCN Std + 27817530 SRV Std

58 cases used, 1582 cases contain missing values

```
Predictor     Coef SE Coef    T    P   VIF
Constant   6476041 22240497 0.29 0.772
MEV Std    34059484 13225820 2.58 0.013 1.197
CKC Std   40624869 21180437 1.92 0.061 1.481
BCN Std   15206424 14794849 1.03 0.309 1.453
SRV Std   27817530 13158860 2.11 0.039 1.346
```

S = 25981129   R-Sq = 40.9%   R-Sq(adj) = 36.5%

PRESS = 4.261470E+16   R-Sq(pred) = 29.62%

Analysis of Variance

```
Source       DF      SS       MS      F    P
Regression    4 2.47732E+16 6.19330E+15 9.18 0.000
Residual Error 53 3.57760E+16 6.75019E+14
Total        57 6.05492E+16
```

```
Source  DF    Seq SS
MEV Std  1  1.05572E+16
CKC Std  1  9.52106E+15
BCN Std  1  1.67833E+15
SRV Std  1  3.01659E+15
```

---

## LTLBG3:

The regression equation is
LTLBG = 28776055 + 38860250 MEV Std + 33003289 SRV  Std + 27733215 BCN  Std

58 cases used, 1582 cases contain missing values

```
Predictor    Coef  SE Coef   T    P   VIF
Constant  28776055 19424144  1.48  0.144
MEV Std   38860250 13305051  2.92  0.005  1.154
SRV Std   33003289 13193676  2.50  0.015  1.289
BCN Std   27733215 13600577  2.04  0.046  1.170
```

S = 26617774   R-Sq = 36.8%   R-Sq(adj) = 33.3%

PRESS = 4.328324E+16   R-Sq(pred) = 28.52%

Analysis of Variance

```
Source       DF      SS       MS      F    P
Regression    3 2.22899E+16 7.42997E+15 10.49 0.000
Residual Error 54 3.82593E+16 7.08506E+14
Total        57 6.05492E+16
```

```
Source   DF    Seq SS
MEV Std  1  1.05572E+16
SRV Std  1  8.78670E+15
BCN Std  1  2.94598E+15
```

---

## TONGE1:

The regression equation is
TONGE = 9025356 - 53450157 ARR  Std + 93134525 CKC  Std + 60119111 MEV Std + 35709887 SRV  Std

56 cases used, 1584 cases contain missing values

```
Predictor    Coef  SE Coef   T    P   VIF
Constant   9025356 22978910  0.39  0.696
```

```
ARR  Std  -53450157  19102200  -2.80  0.007  1.601
CKC  Std   93134525  21189780   4.40  0.000  1.397
MEV  Std   60119111  13261388   4.53  0.000  1.253
SRV  Std   35709887  12799423   2.79  0.007  1.272
```

S = 25316975   R-Sq = 55.7%   R-Sq(adj) = 52.3%

PRESS = 3.857455E+16   R-Sq(pred) = 47.77%

Analysis of Variance

```
Source        DF      SS       MS      F      P
Regression     4  4.11623E+16  1.02906E+16  16.06  0.000
Residual Error 51  3.26884E+16  6.40949E+14
Total         55  7.38507E+16
```

No replicates.
Cannot do pure error test.

```
Source   DF     Seq SS
ARR  Std  1  3.53725E+15
CKC  Std  1  1.57672E+16
MEV  Std  1  1.68687E+16
SRV  Std  1  4.98907E+15
```

---

## TONGE2:

The regression equation is
TONGE = - 25862116 + 57739540 CKC  Std + 44062864 MEV Std + 31522155 SRV  Std + 37827748
TRVLPStd

56 cases used, 1584 cases contain missing values

```
Predictor     Coef  SE Coef    T     P    VIF
Constant   -25862116  26231055  -0.99  0.329
CKC  Std    57739540  20560699   2.81  0.007  1.237
MEV  Std    44062864  12951844   3.40  0.001  1.124
SRV  Std    31522155  13037898   2.42  0.019  1.241
TRVLPStd    37827748  18186876   2.08  0.043  1.094
```

S = 26106212   R-Sq = 52.9%   R-Sq(adj) = 49.2%

PRESS = 4.172715E+16   R-Sq(pred) = 43.50%

Analysis of Variance

```
Source        DF      SS       MS      F      P
Regression     4  3.90924E+16  9.77311E+15  14.34  0.000
Residual Error 51  3.47582E+16  6.81534E+14
Total         55  7.38507E+16
```

No replicates.

Cannot do pure error test.

Source   DF     Seq SS
CKC  Std   1  1.91953E+16
MEV Std    1  1.34170E+16
SRV  Std   1  3.53170E+15
TRVLPStd   1  2.94844E+15

_____

## TONGE3:

The regression equation is
TONGE = 10632286 + 45488796 MEV Std + 43825794 SRV  Std + 50776654 TRVLPStd

56 cases used, 1584 cases contain missing values

Predictor     Coef  SE Coef   T     P   VIF
Constant   10632286  24247512  0.44  0.663
MEV Std    45488796  13772187  3.30  0.002  1.123
SRV  Std  43825794  13067534  3.35  0.001  1.101
TRVLPStd   50776654  18721310  2.71  0.009  1.024

S = 27781082   R-Sq = 45.7%   R-Sq(adj) = 42.5%

PRESS = 4.642206E+16   R-Sq(pred) = 37.14%

Analysis of Variance

Source         DF        SS        MS     F     P
Regression     3  3.37177E+16  1.12392E+16  14.56  0.000
Residual Error  52  4.01330E+16  7.71789E+14
Total          55  7.38507E+16

No replicates.
Cannot do pure error test.

Source   DF     Seq SS
MEV Std    1  1.91319E+16
SRV  Std  1  8.90830E+15
TRVLPStd   1  5.67746E+15

_____

## SHLAB1:

The regression equation is
SHLAB = 2830107 + 9726871 CKC  Std + 9987741 MEV Std + 9695513 TCN  Std

41 cases used, 1599 cases contain missing values

Predictor    Coef  SE Coef    T     P   VIF
Constant   2830107  4740842  0.60  0.554
CKC  Std   9726871  3833670  2.54  0.016  1.109

MEV Std   9987741  2835821  3.52  0.001  1.044
TCN  Std  9695513  2885130  3.36  0.002  1.150

S = 4539865   R-Sq = 55.4%   R-Sq(adj) = 51.8%

PRESS = 9.210870E+14   R-Sq(pred) = 46.14%

Analysis of Variance

Source        DF       SS        MS       F     P
Regression     3  9.47584E+14  3.15861E+14  15.33  0.000
Residual Error 37  7.62584E+14  2.06104E+13
Total         40  1.71017E+15

No replicates.
Cannot do pure error test.

Source   DF     Seq SS
CKC  Std  1  3.45026E+14
MEV Std   1  3.69804E+14
TCN  Std  1  2.32754E+14

---

## SHLAB2:

The regression equation is
SHLAB = 11772642 + 10123890 MEV Std + 11915203 TCN  Std

41 cases used, 1599 cases contain missing values

Predictor     Coef  SE Coef   T     P    VIF
Constant   11772642  3389948  3.47  0.001
MEV Std    10123890  3031389  3.34  0.002  1.044
TCN  Std  11915203  2939419  4.05  0.000  1.044

S = 4853818   R-Sq = 47.7%   R-Sq(adj) = 44.9%

PRESS = 1.036600E+15   R-Sq(pred) = 39.39%

Analysis of Variance

Source        DF       SS        MS       F     P
Regression     2  8.14905E+14  4.07452E+14  17.29  0.000
Residual Error 38  8.95263E+14  2.35595E+13
Total         40  1.71017E+15

No replicates.
Cannot do pure error test.

Source   DF     Seq SS
MEV Std   1  4.27784E+14
TCN  Std  1  3.87121E+14

TENSL1:

The regression equation is
TENSLEXT = 28135053 + 42855642 CKC  Std + 26832984 MEV Std + 16986205 TCN  Std

49 cases used, 1591 cases contain missing values

Predictor    Coef  SE Coef    T     P    VIF
Constant   28135053  12075263  2.33  0.024
CKC  Std   42855642  10631790  4.03  0.000  1.168
MEV Std    26832984   7366494  3.64  0.001  1.241
TCN  Std   16986205   8330319  2.04  0.047  1.362

S = 13465276   R-Sq = 59.3%   R-Sq(adj) = 56.5%

PRESS = 9.247982E+15   R-Sq(pred) = 53.81%

Analysis of Variance

Source        DF        SS        MS      F     P
Regression     3  1.18642E+16  3.95475E+15  21.81  0.000
Residual Error  45  8.15911E+15  1.81314E+14
Total         48  2.00234E+16

No replicates.
Cannot do pure error test.

Source    DF     Seq SS
CKC  Std   1  6.93496E+15
MEV Std    1  4.17541E+15
TCN  Std   1  7.53876E+14

TENSL2:

The regression equation is
TENSLEXT = 65774291 + 29357842 MEV Std + 27353393 TCN  Std

49 cases used, 1591 cases contain missing values

Predictor    Coef  SE Coef    T     P    VIF
Constant   65774291  8834641  7.45  0.000
MEV Std    29357842  8469399  3.47  0.001  1.232
TCN  Std   27353393  9142732  2.99  0.004  1.232

S = 15537557   R-Sq = 44.5%   R-Sq(adj) = 42.1%

PRESS = 1.231929E+16   R-Sq(pred) = 38.48%

Analysis of Variance

```
Source        DF        SS        MS      F      P
Regression     2  8.91824E+15  4.45912E+15  18.47  0.000
Residual Error  46  1.11051E+16  2.41416E+14
Total         48  2.00234E+16
```

No replicates.
Cannot do pure error test.

```
Source    DF      Seq SS
MEV Std    1  6.75733E+15
TCN  Std   1  2.16091E+15
```

APPENDIX E

SELECTED STREAMFLOW STATISTICS

**These data are located on a companion CD.  If a CD is not attached to the back cover of this document, please contact your local or public university library to place an interlibrary loan request to Montana State University.  Please call 406-994-3161 with any questions.

APPENDIX F

DROUGHT RANKINGS

**These data are located on a companion CD.  If a CD is not attached to the back cover of this document, please contact your local or public university library to place an interlibrary loan request to Montana State University.  Please call 406-994-3161 with any questions.

## APPENDIX G

### STREAMFLOW RECONSTRUCTIONS

**These data are located on a companion CD.  If a CD is not attached to the back cover of this document, please contact your local or public university library to place an interlibrary loan request to Montana State University.  Please call 406-994-3161 with any questions.

## APPENDIX H

### SPATIAL DIFFERENCES STATISTICS

**These data are located on a companion CD.  If a CD is not attached to the back cover of this document, please contact your local or public university library to place an interlibrary loan request to Montana State University.  Please call 406-994-3161 with any questions.

## APPENDIX I

### STREAMFLOW-OCEANIC CLIMATE CORRELATIONS

**These data are located on a companion CD.  If a CD is not attached to the back cover of this document, please contact your local or public university library to place an interlibrary loan request to Montana State University.  Please call 406-994-3161 with any questions.

<u>APPENDIX J</u>

UPPER SMITH CREEK CHRONOLOGY

**These data are located on a companion CD.  If a CD is not attached to the back cover of this document, please contact your local or public university library to place an interlibrary loan request to Montana State University.  Please call 406-994-3161 with any questions.

APPENDIX K

BEARTOOTH LOOKOUT CHRONOLOGY

**These data are located on a companion CD.  If a CD is not attached to the back cover of this document, please contact your local or public university library to place an interlibrary loan request to Montana State University.  Please call 406-994-3161 with any questions.